

Review Article

Wan Mohd. Arif Aziz Japar, Nor Azwadi Che Sidik*, Rahman Saidur, Yutaka Asako, and Siti Nurul Akmal Yusof

A review of passive methods in microchannel heat sink application through advanced geometric structure and nanofluids: Current advancements and challenges

<https://doi.org/10.1515/ntrev-2020-0094>

received August 16, 2020; accepted November 19, 2020

Abstract: Microchannel heat sink (MCHS) is an advanced cooling technique to fulfil the cooling demand for electronic devices installed with high-power integrated circuit packages (microchips). Various microchannel designs have been innovated to improve the heat transfer performance in an MCHS. Specifically, the utilisation of nanotechnology in the form of nanofluid in an MCHS attracted the attention of researchers because of considerable enhancement of thermal conductivity in nanofluid even at a low nanoparticle concentration. However, a high-pressure drop was the main limitation as it controls the MCHS performance resulted from heat transfer augmentation. Therefore, this study aimed to critically summarise the challenges and limitations of both single and hybrid passive methods of MCHS. Furthermore, the performance of nanofluid as a coolant in the MCHS as affected by the type and concentration of nanoparticle and the type of base fluid was reviewed systematically. The review indicated that the hybrid MCHS provides a better cooling performance than MCHS with the single passive method as the former results in a higher heat transfer rate with minimal pressure drop penalty. Besides that, further heat transfer performance can be enhanced by dispersing aluminium dioxide (Al_2O_3) nanoparticles

with a concentration of less than 2.0% (v/v) in the water-based coolant.

Keywords: thermal management, convective heat transfer, microchannel heat sink, passive design, nanotechnology, nanofluid

1 Introduction

Application of cooling system in thermal engineering is recognised and have been studied both theoretically and practically in building energy system, electronic devices, chemical vapour deposition instruments, solar energy collectors, furnace engineering, and many more [1]. In recent years, thermal management of electronic devices is of interest as a new generation of high performing dense chip packages that function at high frequency produces a very high heat flux on the electronic devices. Prolonged heat flux creates a hot spot on the electronic devices and reduces the lifespan of the electronic devices because of the acceleration of the mean time to failure (MTTF) as described by the Black's equation [2]. Thermal management of compact electronic devices that operate at high power density is critical as there is a lack of efficient technique to remove heat dissipation from the electronic devices [3]. The increase in power density and miniaturisation of electronic packages have changed the direction of cooling system technology, from air-cooling technology to advanced heat transfer technology because of the inadequacy of conventional method to remove extreme high heat flux [4].

Several methods have been proposed in the previous studies to improve the cooling performance, such as air cooling method [5], heat pipe method [6], use of liquid material as a coolant [7], and micro-cooling method [8]. Micro-cooling is a good technique because of its high cooling efficiency compared to the other methods. Even though the air cooling method is the simplest cooling technique, it has a low cooling efficiency with additional heat generation by the fan itself [9]. Meanwhile, for the

* **Corresponding author: Nor Azwadi Che Sidik**, Malaysia – Japan International Institute of Technology (MJIT), Universiti Teknologi Malaysia Kuala Lumpur, Jalan Sultan Yahya Petra, 54100 Kuala Lumpur, Malaysia, e-mail: azwadi@utm.my

Wan Mohd. Arif Aziz Japar, Yutaka Asako, Siti Nurul Akmal Yusof: Malaysia – Japan International Institute of Technology (MJIT), Universiti Teknologi Malaysia Kuala Lumpur, Jalan Sultan Yahya Petra, 54100 Kuala Lumpur, Malaysia

Rahman Saidur: Research Centre for Nano-Materials and Energy Technology, School of Science and Technology, Sunway University, Bandar Sunway, 47500 Subang Jaya, Selangor, Malaysia; Department of Engineering, Lancaster University, Lancaster LA1 4YW, United Kingdom

liquid material and heat pipe applications, space is required to accommodate additional system for condensation process [9], which is not suitable for compact electronic devices. Therefore, the micro-cooling method is one of the promising techniques that can dissipate a very high heat flux generated by the compact electronic devices that can be attributed to the high heat transfer surface-area-to-volume ratio. Besides that, the micro hydraulic diameter also contributes to the heat transfer performance enhancement because of the augmentation of heat transfer coefficient [10]. When the micro-cooling method was used, microchannel heat sink (MCHS) was found to be the most prospective as a very high heat flux can be removed compared to micro-jet impingement, micro-heat pipe, and micro-electro-hydrodynamic methods [11]. In 1981, Tuckerman and Pease [12] reported that rectangular MCHS can remove heat-flux up to 790 W/cm^2 . However, the pumping power required by the MCHS was very high because of high-pressure drop penalty generated in the microchannel. Based on the study of Japar et al. [13], high-pressure drop penalty was attributed to high wall shear stress in the developing region of laminar flow. The discovery motivated many scholars to investigate the performance of rectangular microchannel via geometry parameter and stacked layer optimisations.

Khan et al. [14] stated that when the aspect ratio of a rectangular microchannel (channel width to channel height) increased, thermal and hydraulic resistances decreased because of the larger convective heat transfer area and flow cross-section area, respectively. The findings were further supported by Kowsari et al. [15] where for a smaller and constant cross-section area, the heat transfer performance increased with channel aspect ratio. In-depth effect of a rectangular channel aspect ratio on the thermal performance was investigated by Sobhan et al. [16] and Kou et al. [17]. The authors found that at a fixed aspect ratio, channel width significantly affected thermal resistance as the bottom channel area lied directly under the applied heat flux. Besides the thermal resistance issue, the pressure drop penalty was also an aim of rectangular channel MCHS optimisation process. One of the related studies includes investigation of hydrothermal performance in a single-layered and double-layered MCHS to reduce the pressure drop penalty by Chong et al. [18]. The study reported that in the laminar region, the double-layer MCHS reduced the pressure drop by 53.9% compared to the single-layered MCHS. However, the thermal resistance in the double-layered MCHS was higher than the single-layered MCHS by 20.8%. A solution was proposed by Wei and Joshi [19] to reduce the thermal resistance in a stacked MCHS, either by increasing the pumping power or

by reducing the channel length. Hung and Yan [20] also recommended increasing the pumping power to mitigate the optimal thermal resistance. However, in another novel study by Wang et al. [21], both thermal resistance and pumping power consumption were improved simultaneously through optimisation of semi-porous rib geometry. The researchers reported that the double-layered MCHS with the optimised semi-porous-rib geometry improved the cooling performance and pumping power by 14.06% and 16.40%, respectively.

Nevertheless, further geometry optimisation of a rectangular channel MCHS was limited by pressure drop penalty in a monolayer MCHS and additional space requirement by a multilayer MCHS in the cooling system of a compact electronic device. In recent years, nanotechnology was applied to further improve the performance of hydrothermal. According to Nanotechnology journal database, nanotechnology is widely used in various fields such as medical [22–24], biomedical especially for cancer detection [25–27] and treatment [28,29], bone regeneration [30–32], vaccine [33] and drug [34] delivery system, central nervous system [35], biological imaging [36], and membrane proteins analysis [37,38]. However, studies on the nanofluid application for thermal management [39] are limited.

Recently, many investigations were conducted to enhance the performance of MCHS through advanced geometric structure and nanofluid [40], which can provide high thermal performance with an acceptable pressure drop. Adham et al. [41] presented a review on the effect of constant cross-section shape on hydrothermal performance to provide a better understanding of research related to geometric structure. Simple cross-section channels such as rectangular, trapezoidal, triangular, and square shapes were reviewed to find a suitable flow condition and performance indicator for MCHS application. In another review by Kumar et al. [42], nanofluid behaviour in various shapes of MCHS was discussed. Based on both the reviews, the best shape of MCHS that has a higher thermal performance and a lower friction loss was suggested. However, the difference in performance between a hybrid MCHS (the combination of more than one passive method) and single passive method of MCHS was not included in both the reviews. Besides, the range of nanoparticle concentration, type of nanoparticle, and base fluid that are commonly used in MCHS application were also not discussed in both reviews, and hence the details are presented in the current review. Therefore, the challenges and limitations of single passive and hybrid passive methods that were adopted in micro-channel designs are discussed critically in the present

review based on the respective geometry structure and mechanism.

2 Hydrothermal performance enhancement technique

For the past 30 years, many methods were proposed to improve the overall performance of MCHS with minimal thermal resistance and pressure drop that can satisfy the cooling demand. Generally, the methods can be categorised into two groups namely active and passive. The active method uses external energy in the system to improve the heat transfer performance, whereas the passive method does not require external energy. In general, the passive method was preferred because of its low cost and absence of mechanical moving part compared to the active method. Figure 1 shows the techniques used as part of the active method [43–49] and passive method [50–88] that are available in the open literature.

2.1 Active method

Since the middle of 1981, majority of studies emphasised on the passive method than the active method in the performance enhancement of MCHS because of the compact design of advanced electronic devices. However, few researchers attempted to improve heat transfer performance using the active method. In 2003, Go [43] evaluated the effect of flow-induced vibration of a microfin array on heat transfer augmentation. The study reported that the high heat transfer rate was obtained by increasing

the vibration displacement of the microfin. In another innovative work, Krishnaveni *et al.* [46] proposed a periodic electric field technique in rectangular MCHS where chaotic mixing in a microchannel was induced which contributed to heat transfer augmentation. In a different study, Hessami *et al.* [47] reported on the effect of flow pulsation technique on microchannel performance and concluded that heat transfer enhancement was obtained by increasing the frequency and reducing the amplitude of flow pulsation. Variable roughness structure technique is not popular and least studied, which could be because of the complexity of the system designed for the compact area.

2.2 Passive method

2.2.1 MCHS with single/individual passive method

Single/individual passive method of MCHS refers to a design that implements only one of the passive methods in its channel design with less complex geometry structure in contrast to the hybrid design MCHS. However, this single passive method of MCHS is only efficient at low Reynolds number (Re) because of high-pressure drop penalty at higher Re as shown in Table 1. There are three main factors that contribute to the enhancement of the heat transfer performance in the single passive method of MCHS, namely high degree of fluid mixing, mainstream flow separation, and the periodic break-up of the boundary layer (Table 1). These flow mechanisms can be caused by the Dean vortices formation, secondary flow generation, jet and throttling effect, and the entrance effect. It is worth stating here that the aforementioned flow behaviours assist in the enhancement of heat transfer performance besides the convective heat transfer area factor.

According to Bhandari and Prajapati [89], pin fin height affects the heat transfer performance because of Dean vortices formation. The study reported that the enhancement of heat transfer performance in the microchannel with a fin height of 1.5 mm (convective surface area: 639 mm²) was higher when compared with a fin height of 2.0 mm (convective surface area: 687 mm²). The vortices formation increased the effective area of convective heat transfer. In another novel study [90], the formation of Dean vortices in microchannels was reported to reduce the boundary layer thickness and provide a more uniform velocity distribution along the microchannels.

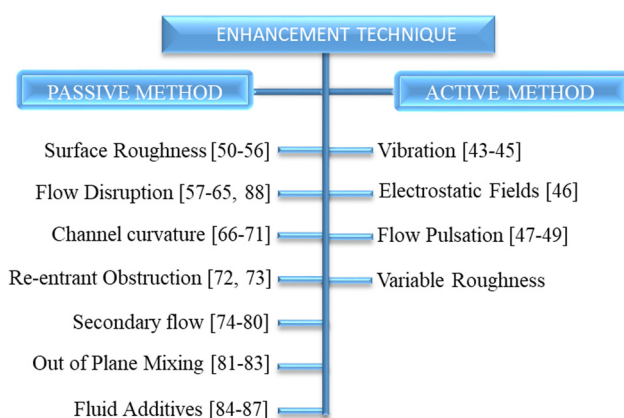


Figure 1: Enhancement technique for MCHS.

Table 1: Performance of MCHS with single/individual passive method

Flow disruption		
Author: Hong and Cheng (2009) [57]	Geometry structure: Offset strip-fin microchannels	Re: 75
Optimum geometry parameter: The ratio of fin interval to fin length is 1		
Observations: (1) The heat transfer coefficient increases with the number of fins as the flow disturbance and break-up of the boundary become more frequent; (2) heat transfer area increases with the number of fins; (3) lower flow rate is required as a higher number of fins provides a higher heat transfer rate; (4) the optimum number of fins is vital to prevent the higher pressure drop penalty		
Author: Chai et al. (2013) [58]	Geometry structure: Interrupted microchannel with rectangular ribs in the transverse microchambers	Re: 187–715
Optimum geometry parameters: For $Re < 400$: Rectangular rib width (w): 0.14 mm; rectangular rib length (l): 0.5 mm; the distance from the parallel microchannels to the rib row, $d = 0.2$ mm and 0.25 mm; the space between two adjoining transverse microchambers, $s = 1.3$ mm		
Observations: (1) The rib length and width have a significant effect on heat transfer performance; (2) the friction factor and heat transfer rate increased with the length and width of ribs geometry; (3) the friction factor augmentation was more affected by the rib width than the rib length; (4) the friction factor and heat transfer rate were more affected by the space between two adjacent transverse microchambers, s , than the distance from the parallel microchannels to the rib row, d		
Author: Chai and Wang (2018) [61]	Geometry structure: Interrupted MCHSs with different rib geometries in transverse microchambers (rectangular, backward triangular, diamond, forward triangular, and ellipsoidal ribs)	Re: 187–715
Optimum geometry parameter: The ellipsoidal ribs with the length of 0.5 mm showed the best overall performance		
Observations: (1) Ribs geometry with a flat surface at the leading edge perpendicular to the mainstream produced a high friction factor; (2) the effect of rib length on the friction factor augmentation depends on the shape of ribs geometry		
Author: Xie et al. (2014) [59]	Geometry structure: MCHSs with different multistage bifurcations	Re: 230–560
Optimum geometry parameter: Single-stage bifurcation with long bifurcation plate (length: 25 mm; width/thickness: 35 μ m)		
Observations: (1) Uniform temperature distribution at the heated wall; (2) pressure drop augmentation in the MCHS with multistage bifurcations was affected by bifurcation plates length close to the channel exit; (3) two-stage bifurcations were the optimum stage number in the MCHS with multistage bifurcation design; (4) the pressure drop augmentation increased with the number of bifurcation plate because of the enhancement of fluid velocity in the smaller channel		
Channel curvature		
Author: Sui et al. (2010) [66]	Geometry structure: Wavy microchannel with the rectangular cross-section	Re: 100–800
Optimum geometry parameter: Wavy microchannel with a relative wavy amplitude from 0.05 to 0.125		
Observations: (1) The heat transfer performance and pressure drop penalty increased with increasing relative wavy amplitude of microchannel; (2) the optimum relative amplitude of the wavy channel is essential to prevent high-pressure drop penalty that dominates the heat transfer performance augmentation; (3) at a fixed relative wavy amplitude, the number of Dean vortices formation increased with the Re ; (4) stretching and folding of fluid-particle generated by several Dean vortices promoted a higher degree of flow mixing		
Author: Mills et al. (2016) [67]	Geometry structure: Microchannel with the wavy-walled channel	Re: $Re < 800$
Optimum geometry parameters: For $280 < Re < 385$: (1) The ratio of wall amplitude to the distance between sidewalls, A , was 0.35; (2) the ratio of wall oscillation period to the distance between the sidewall and the centre line of the microchannel, L , was 3. For $Re > 385$: (1) The ratio of wall amplitude to the distance between sidewalls, A , was 0.25; (2) the ratio of wall oscillation period to the distance between the sidewall and the centre line of the microchannel, L , was 3		
Observations: (1) The amplitude of wall waviness was more effective at a lower flow rate in a steady regime for heat transfer performance enhancement; (2) heat transfer performance augmentation in an unsteady regime was higher than in a steady regime; (3) heat transfer enhancement in an unsteady region was influenced more by the pressure drop than the wall amplitude; (4) the formation of Dean vortices in an unsteady regime was more effective than in a steady regime for heat transfer performance enhancement		
Author: Lin et al. (2017) [68]	Geometry structure: MCHS with a wavy channel	Re: 300–800
Optimum geometry parameters: Two adjacent wavy geometries with the wavelength and amplitude difference of 400 and 8 μ m, respectively		
Observations: (1) The amplitude and wavelength of wavy geometry have a significant impact on the thermal resistance and bottom wall temperature; (2) low thermal resistance and small temperature difference at the bottom wall can be obtained by increasing the wave amplitude and reducing the wavelength of wavy geometry; (3) greater Dean vortices formation at the channel inlet can be obtained by increasing the wavy wavelength and reducing the wave amplitude; (4) greater Dean vortices formation at the channel outlet can be obtained by reducing the wavy wavelength and increasing the wave amplitude; (5) superior thermal performance can be achieved by increasing the wavelength or amplitude difference between two adjacent wavy geometries with small aspect ratio		

Table 1: Continued

Secondary flow		
Author: Lee et al. (2012) [74]	Geometry structure: Microchannel with oblique fins	Re: 300–800
Optimum geometry parameter: The oblique angle was 27°		
Observations: (1) Diversion of the mainstream to a small fraction of flow into adjacent main channels; (2) a thinner boundary layer zone formation was related to fluid fraction flow from the main channel to the secondary channel; (3) the oblique fin geometries increased the heat transfer area and subsequently enhanced the heat transfer rate which also increased the pressure drop; (4) the thermal boundary layer decreased with increasing Re; (5) the existence of a secondary channel provided by the oblique geometry further improved the heat transfer performance by disrupting the mainstream of adjacent main channel; (6) high pumping power was required to divert a greater amount of flow into the secondary channel with a stronger momentum which increased the heat transfer performance with excessive pressure drop penalty noted; (7) smaller fin pitch increased the intensity of boundary layer development; (8) smaller oblique angle increased secondary flow into the secondary channel		
Author: Lee et al. (2015) [77]	Geometry structure: Microchannel with oblique fins	Re: 180–680
Optimum geometry parameters: Hydraulic diameter, oblique angle, and fin pitch were 104 μm , 27°, and 400 μm , respectively		
Observations: (1) The thermal resistance in the enhanced microchannel decreased rapidly with the increase in Re; (2) oblique fin geometries provided a more uniform temperature distribution but increased the pressure drop; (3) the high-pressure drop was generated after Re achieved 500		
Author: Kuppusamy et al. (2014) [75]	Geometry structure: Microchannel with the slanted secondary channel in alternating orientation	Re: N/A
Optimum geometry parameters: The secondary channel width (α), length of the longer edge of the fins (β), and secondary channel angle (θ) were 64, 160 μm , and 37°, respectively		
Observations: (1) Presence of secondary channels in alternating orientation enhanced the heat transfer performance, besides reducing pressure drop in the enhanced microchannel; (2) heat transfer rate increased with the width of the secondary channel; (3) thermal resistance and pressure drop decreased with increasing secondary channel width; (4) heat transfer rate increased with decreasing longer edge length of fins and secondary channel angle; (5) thermal resistance and pressure drop decreased with a longer edge length of fins and secondary channel angle		

Among the passive methods, surface roughness [50,51,55] and re-entrant obstructions [72] got less attention by previous researchers. Geometry parameter in the surface roughness method is difficult to control during fabrication process to get the uniform surface roughness. The relative height of roughness affects the size of the vortex flow formation adjacent to the roughness element. The larger the vortex flow formation size, the weaker the heat transfer performance [55]. Besides that, the surface roughness method is only more effective at the higher heat flux [51], fluid temperature, and heating power [50]. For the re-entrant obstructions method, high-pressure drop penalty is produced because of the entrance effect influenced by constriction–expansion geometry [72].

2.2.2 MCHS with hybrid passive method

Numerous studies and reviews were carried out to explore the potential of a single passive method for microchannel design innovation compared to hybrid passive method because of the less complex geometry of the former. However, high-pressure drop issue is the main constrain of single passive method of MCHS. To minimise pressure drop and increase the heat transfer performance, hybrid passive method of MCHS which use more than one passive method in its channel design is of growing interest.

Recently, many researchers have used the hybrid passive method in a single-phase flow for the enhancement of MCHS performance. In 2020, van Erp et al. [91] reported a sustainable enhanced MCHS with three important solutions: (1) high cooling performance; (2) less water and energy consumption; and (3) small and compact heat sink. Li et al. [92] proposed a novel high-efficiency-low-resistance heat exchanger design. The study reported that the combination of the dimple and pin-fin geometries used in the design provided a higher heat transfer rate with energy-saving and low resistance features enhanced the thermal performance by 10.3% at a Re of 200. Besides, the area of the high-temperature region and temperature gradient decreased. Furthermore, the violent action of flow on the heated wall provided by pin-fin increased the uniformity of the heated area.

In 2013, Gong and Wei [93] analysed the performance of microchannel structured by dimple and wavy shapes where the effect of dimple number in the wavy wall was studied numerically. The presence of the dimple structure in the wavy channel was reported to enhance the heat transfer performance but not the flow resistance. Besides, the overall performance of microchannel was enhanced with increasing dimple number. In a subsequent study in 2016, Gong et al. [94] investigated similar geometry combination with different orientation of dimple structure. The experimental findings showed that microchannel

with dimple structures in the throat of the wavy channel has the best thermal performance compared to dimple structure in the cavity of the wavy channel. The dimple structure in the cavity area reduced the overall performance provided by the wavy channel as the velocity gradient reduced on the contact surface.

A year later, in 2017, the performance of convergent-divergent channel with ribs and cavities on the sidewall was reported by Srivastava et al. [95] for constant heat flux and Re of 120–900. The findings showed that the developed design reduced the overall thermal resistance up to 40% and the temperature of the microchannel bottom surface was relatively uniform. The combined effect of interruption, redevelopment of the boundary layer, and recirculation zone increased the average Nusselt number from 15% to 46% which contributed to the heat transfer augmentation. However, the overall performance of MCHS decreased when the flow rate was increased because of high-pressure drop penalty.

In recent years, the combined effects of cavities and ribs, on the sidewalls and the centre of the straight channel respectively, have gained more attention. Li et al. [96] presented a numerical study to investigate the effects of ribs and cavities on fluid flow and heat transfer characteristics for the Re of 173–635. Thermal enhancement factor and entropy generation number augmentation were used as the performance indicator. The analysis revealed that combined effect of interruption, redevelopment of the thermal boundary layer, intensified mainstream disturbance, and chaotic mixing between hot and cold water enhanced the heat transfer performance. After a year, Li et al. [97] extended their research using various shapes of ribs and cavities in a straight microchannel, and the rib shapes were found to influence thermal and hydraulic performances to a greater extent. Meanwhile, the triangular ribs showed the lowest heat transfer performance compared to other designs, although it has the lowest pressure drop penalty because of delayed separation point of the mainstream on the triangular geometry. In contrast, the rectangular rib design has the highest pressure drop penalty among all the designs compared. In the same year, Ghani et al. [98] reported that heat transfer augmentation with a minimal pressure drop in a microchannel with sinusoidal cavities and rectangular ribs can be achieved by geometrical optimisation. The optimum relative cavity amplitude, rib width, and rib length found in the study were 0.15, 0.13, and 0.5, respectively. The combination of these optimum parameters resulted in the highest performance factor compared to other designs studied.

In contrast to the aforementioned design configuration, Xia et al. [99,100] analysed the effects of ribs and cavities at the sidewalls on heat transfer performance using two different methods, namely computational fluid dynamics (CFD) and CFD with multi-objective evolutionary algorithm (MOEA). In the CFD method, the analysis found that a relative rib height significantly affected entropy generation. Not only that, the combined effect of flow mixing and redevelopment of the boundary layer in the microchannel increased the heat transfer performance. From the data obtained, Xia et al. [99,100] established a correlation between Nusselt number and friction factor as shown in equations (1) to (3). Meanwhile, in CFD with MOEA method, the result illustrated that relative rib height increased, thermal resistance and pressure drop penalty decreased and increased, respectively. The relative cavity height and rib height exhibited similar performance trend except for the very deep cavities that could be influenced by the formation of a stagnant zone. Besides, MOEA results indicated a relationship between total thermal resistance and pumping power.

$$\begin{aligned} Nu &= 0.495 Re^{0.6371} (e_1/D_h)^{-0.0008} (e_2/D_h)^{0.4166}, \\ 0 < e_1/D_h &\leq 0.65, \\ 0 < e_1/D_h &\leq 0.2167, \end{aligned} \quad (1)$$

$$\begin{aligned} f &= 90.0033^{-0.6629} (e_1/D_h)^{-0.0006} (e_2/D_h)^{0.8854}, \\ 0 < e_1/D_h &\leq 0.65, \\ 0 < e_1/D_h &\leq 0.0848, \end{aligned} \quad (2)$$

$$\begin{aligned} f &= 855.0918^{-0.6} (e_1/D_h)^{-0.0023} (e_2/D_h)^{2.2078}, \\ 0 < e_1/D_h &\leq 0.65, \\ 0 < e_1/D_h &\leq 0.2167. \end{aligned} \quad (3)$$

For a better understanding of the effect of geometry configuration or arrangement of ribs and cavities in the straight channel on the thermal performance, Xie et al. [101] developed several designs to analyse the best configuration of rib and cavity combinations. The highest Nusselt number ratio was obtained when using the configuration of ribs on both sidewalls. The Nusselt number ratio decreased according to the following combinations: cavities and ribs on opposite sidewalls > ribs on the sidewall > cavities on the sidewall. For friction factor ratio, ribs on the sidewall and ribs on both sidewalls exhibited the highest values when compared with other configurations. In general, different types of rib and cavity arrangement could enhance the heat transfer performance compared to a straight microchannel design. However, from the viewpoint of energy saving, the arrangement of the ribs and cavities is very important to prevent a high-pressure drop.

The combination of secondary channel and rib geometries is one of the novel designs which could increase the flow mixing and redevelopment of the boundary layer. The combination of the geometries was applied by Ghani *et al.* [102] to investigate the performance of combined effect on the fluid flow and heat transfer characteristic for the Re of 100–500. The key strategies that were considered in developing a novel design include reduction in pressure drop, the increment of flow mixing, and interruption of main flow for redevelopment of the boundary layer. Optimum parameters for the design were suggested by the authors to achieve maximum thermal performance with a minimal pressure drop penalty.

Another novel design using impinging jet with a dimple structure showed great potential in thermal performance enhancement. Dimple structure design development of an MCHS is important as dimple could increase or decrease the overall performance of the MCHS. Huang *et al.* [103] studied the effect of various shapes of dimples on the fluid flow and heat transfer characteristics in an impinging jet microchannel where convex dimple showed the highest performance enhancement compared to mixed dimples and concave dimple. The presence of convex dimple structure decreased the flow resistance in the microchannel resulting in a lower pumping power consumption. In 2018, similar geometries were analysed by Ming *et al.* [104,105] to determine the optimum geometry parameter of the convex dimple to reduce the heat flux up to 500 W/cm².

Overall, the studies highlight the potential of the combined technique of passive method in a single channel. It was noted that the combined effect from each technique in a passive method resulted in a significant impact on the thermal performance of an MCHS. However, the high-pressure drop issue that affected the pumping power consumption requires consideration in the design development to ensure that the overall performance of MCHS can be improved and optimised. Table 2 shows the summary of current designs [92–103,106–110], challenges, and limitations of MCHS with hybrid passive method.

It is worth mentioning here that the combination of more than one passive methods in a microchannel design can improve or negatively affect the overall performance of MCHS. According to Lu *et al.* [113], the effect surface roughness of three different microchannel designs, namely wavy, dimpled, and square channels on hydrothermal performance, was highly dependent on the local flow field in each design. The surface roughness has a less impact on the dimpled and valley of the wavy channel because of low-velocity area present close to the wall.

However, in another study, Yang *et al.* [114] reported that the hybrid MCHS showed superior hydraulic performance over the wide range of Re ($Re < 883$) compared to the single passive design MCHS. Li *et al.* [115] also portrayed a similar trend in the overall performance of hybrid MCHS. The authors found that MCHS with isosceles triangular cavities and forward drop-shaped fins resulted in a high thermal performance improvement with a relatively small flow resistance.

Besides out of plane mixing method, secondary flow generated by a secondary channel is an alternative method, which can provide a high degree of flow mixing with a relatively small flow resistance. The effectiveness of secondary channel geometry was reported numerically in our previous research [111]. The study showed that the existence of secondary channel geometry in hybrid MCHS (TC-RR-SC MCHS) increased the degree of flow mixing between cold and hot water in the main microchannel and adjacent microchannel. Besides that, the design also resulted in the reduction in pressure drop by providing a large flow area for coolant. Model for hybrid MCHS with secondary channels is as shown in Figure 2. This design appears as the best hybrid MCHS compared to our other designs [116–119] because it increases the cooling performance, reduces the water-coolant and pumping power consumption, and small and compact in size.

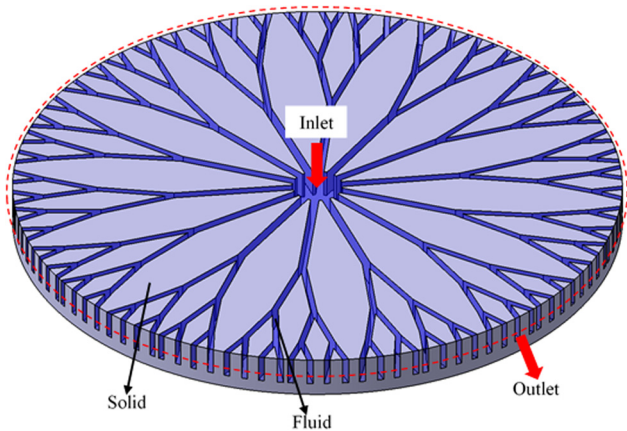
2.2.3 Utilisation of nanofluid in an MCHS with passive design

In the last decade, many researches were performed to innovate the design of flow passage to enhance MCHS performance. However, some studies focused on increasing the heat transfer performance by improving the transport properties such as fluid thermal conductivity in an MCHS. Continuous discovery of new coolant can improve the ability of convective heat transfer in an MCHS application. Earlier, researchers dispersed solid particle of micrometre and millimetre size in a water-based fluid to improve the thermal conductivity that can enhance the heat transfer performance. Practical limitations of the method are well established and the most common drawback was the clogging effect. In 1995, Choi and Eastman [120] introduced a new advanced potential coolant named nanofluid. Nanofluid is being used widely as a coolant additive in the MCHS application. Nanofluid is usually prepared by dispersing solid particles with nanometre size in a base fluid.

Table 2: Advanced structure, challenges, and limitations of passive methods in a microchannel

Yan et al. [106]

Design: Secondary flow and flow disruption methods



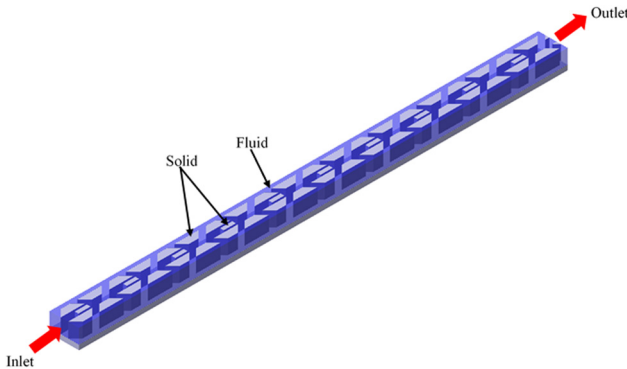
Overall performance: The coefficient of performance ratio ((COP)_r) was 0.97 at flow rate of 400 mL/min

Challenges and limitations:

- The maximum temperature was 347.4 K for heat flux of 100 W/cm² (allowable temperature for semiconductor component < 358.15 K)
- The geometry parameter needs to be optimised for the application that generates a heat flux of more than 100 W/cm². The geometry optimisation (angle and channel width) should be conducted for branch 1 and 2 geometries that have a higher temperature distribution than other areas

Bahiraei et al. [107]

Design: Fluid additive, secondary flow, and flow disruption methods



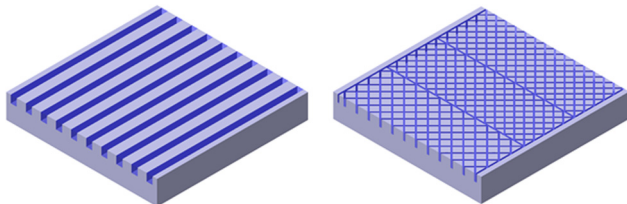
Overall performance: The performance evaluation criteria (PEC) was about 1.15 at a Re of 100

Challenges and limitations:

- Heat transfer performance was more affected by nanoparticle concentration at a lower Re. At a higher Re, nanoparticle concentration had no significant effect on the heat transfer performance
- Lower fluid velocity at dead zone areas (secondary channel and rib downstream) increased the wall temperature at the dead zone areas

Haziq et al. [108]

Design: Secondary flow and flow disruption methods



Overall performance: Thermal resistance decreased by 68%; pressure drop increased by 900%

Challenges and limitations:

- The effect of fin transverse angle is not considered in the optimisation of geometry parameter. The fin transverse angle will give a significant impact on fluid flow and heat transfer characteristics

Table 2: Continued

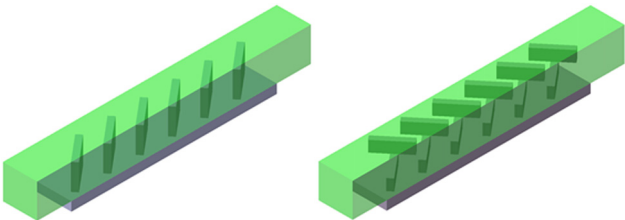
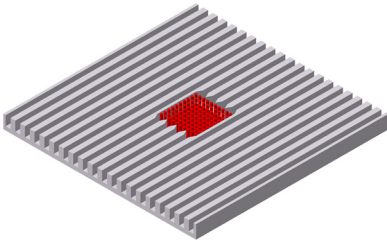
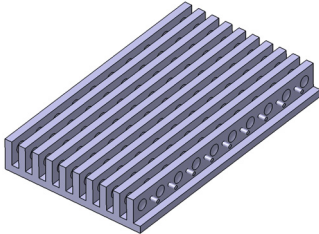
Rui et al. [109]	<p>Design: Surface roughness and flow disruption methods</p>  <p>Overall performance: Highest Nusselt number ratio and friction factor ratio of the proposed designs were about 2.8 and 9, respectively, at a Re of 600</p> <p>Challenges and limitations:</p> <ul style="list-style-type: none">• Optimisation process focused on single-objective optimisation method by fixing the pumping power• The parallel orientation of slant ribs between the top wall and the bottom wall is not considered in the geometry optimisation
Danish et al. [110]	<p>Design: Flow disruption and re-entrant obstruction methods</p>  <p>Overall performance: Thermal performance and pumping power increased by 30.6 and 11.7%, respectively</p> <p>Challenges and limitations:</p> <ul style="list-style-type: none">• The effect of pin fin geometry parameters, namely pin fin shape, and distance between pin fins are not considered in performance analysis
Li et al. [92]	<p>Design: Flow disruption and surface roughness methods</p>  <p>Overall performance: The PEC of the proposed design was 2.12 at a Re of 300</p> <p>Challenges and limitations:</p> <ul style="list-style-type: none">• The design focused only on the low range of Re• Optimum thermal performance could not be determined because of the low range of Re analysis

Table 2: Continued

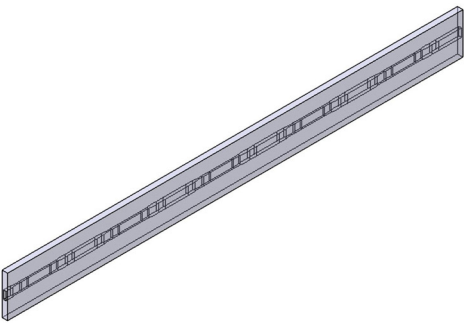


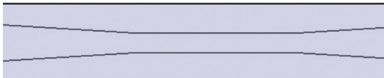
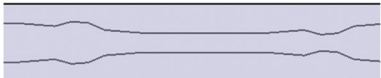
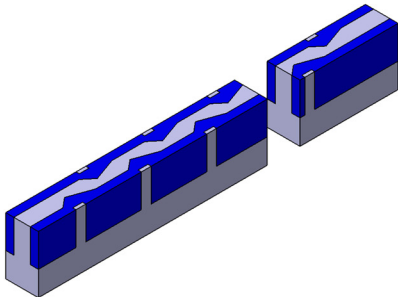
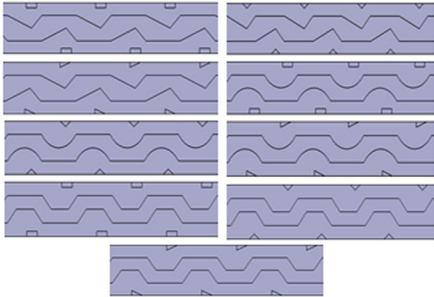
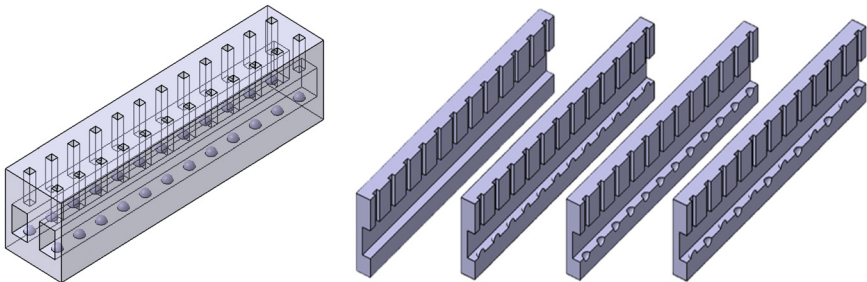
Srivastava et al. [95]	Design: Surface roughness, flow disruption, and re-entrant obstruction methods
<div data-bbox="475 314 1315 959"> <p>(a) Straight Channel</p><p>(b) Rib and cavities</p><p>(c) Convergent-divergent</p><p>(d) Convergent-divergent, rib and cavities</p></div> <p>Overall performance: Overall thermal resistance decreased by 40%</p> <p>Challenges and limitations:</p> <ul style="list-style-type: none">• The applied heat flux was less than 100 W/cm²• The convergent-divergent MCHS with rib and cavity resulted in a superior performance than other designs. However, the design was more effective at a lower range of Re because of a higher pressure drop generated in the design	
Li et al. [97]	Design: Flow disruption, re-entrant obstruction, and surface roughness methods
<div data-bbox="467 1176 1326 1474"> </div> <p>Overall performance: The PEC of all analysed designs in the study were less than 1.46 at a Re of 300–400</p> <p>Challenges and limitations:</p> <ul style="list-style-type: none">• The optimum geometry parameters are not determined because the geometry parameter optimisation is not conducted in the study• Net temperature gradient analysis was used to evaluate the reduction in irreversible heat transfer where the irreversibility process can occur because of friction loss. Therefore, entropy generation analysis [111] that consider both heat transfer and friction loss irreversibility are more suitable for the calculation of total entropy generation in the analysed designs	

Table 2: Continued

Huang et al. [103]

Design: Flow disruption and surface roughness methods



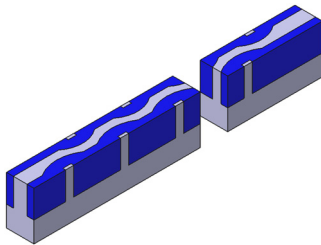
Overall performance: Highest overall performance enhancement of enhanced design was about 15%

Challenges and limitations:

- The analysis of the proposed design focused only on the effect of dimple shapes such as concave and convex shape on the fluid flow and heat transfer characteristics. Overall performance of the proposed design could be enhanced by dimple geometry parameter optimisation. Dimple size can increase the area of heat transfer. Besides that, the degree of flow mixing can also be improved by dimple arrangement in an impinging jet MCHS

Ghani et al. [98]

Design: Flow disruption, re-entrant obstruction, and surface roughness methods



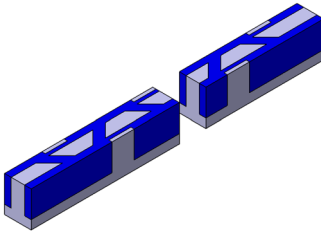
Overall performance: The PEC of the proposed design was 1.85 at a Re of 800

Challenges and limitations:

- The wavelength of sinusoidal cavities was not considered for geometry optimisation
- The only alternate orientation of sinusoidal cavities was analysed in the study. A series of cavity geometry orientation before the alternate orientation can affect the overall performance. This could be because of the heat transfer enhancement by rib geometry without cavity geometry which generates the jet effect

Ghani et al. [102]

Design: Flow disruption and secondary flow methods



Overall performance: The PEC of the proposed design was 1.98 at a Re of 500

Challenges and limitations:

- The length of rib geometry was not considered in geometry optimisation. The length of rib geometry will give a significant impact on the length of flow obstruction, which can further enhance thermal performance [112]

Xia et al. [100]

Design: Flow disruption, re-entrant obstruction, and surface roughness methods

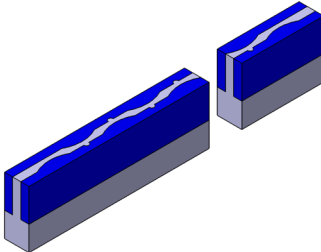


Table 2: Continued

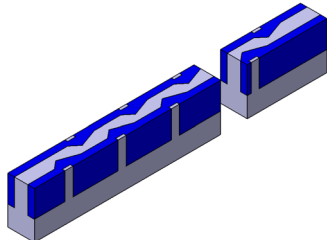
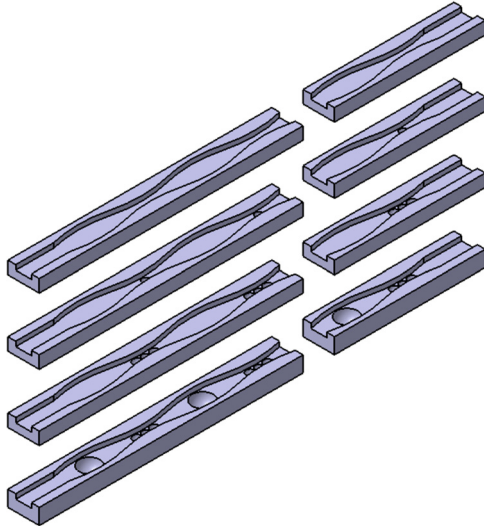
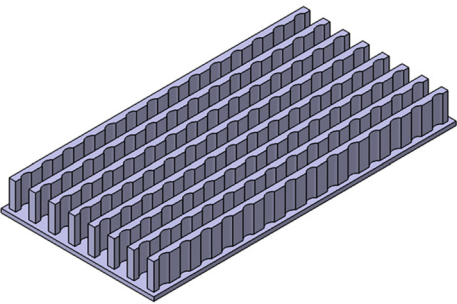
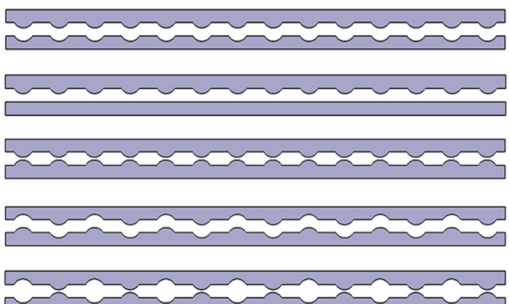
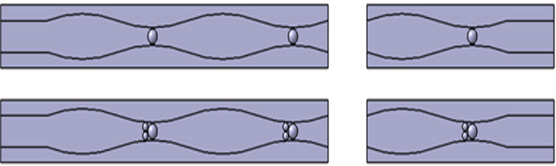
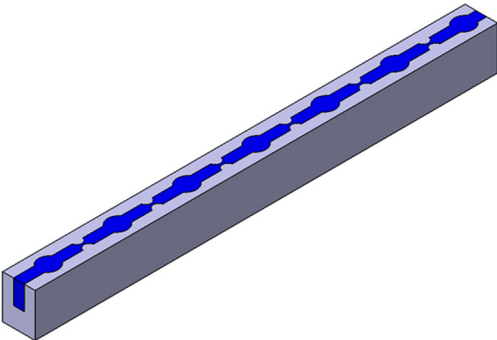
	<p>Overall performance: The lowest thermal resistance was 0.18 K/W at the pumping power of 0.3 W</p> <p>Challenges and limitations:</p> <ul style="list-style-type: none">• The shape of rib geometry plays an important role to improve the overall performance of the MCHS. Further analysis with different rib shapes will provide an idea for design development. For example, rectangular ribs can provide a very effective blocking effect than other designs because of the early separation point of the mainstream in microchannel [97]. Rectangular ribs, in general, do not require higher ribs as required by round ribs
Li et al. [96]	<p>Design: Flow disruption, re-entrant obstruction, and surface roughness methods</p> 
	<p>Overall performance: The PEC of the proposed design was 1.62 at a Re of 500</p> <p>Challenges and limitations:</p> <ul style="list-style-type: none">• Heat at the corner area of cavities cannot be removed efficiently because of the residence time of fluid to remain longer in the stagnation zone (dead zone) area
Gong et al. [94]	<p>Design: Re-entrant obstruction and surface roughness methods</p> 
	<p>Overall performance: Thermal resistance decreased by 60% and pumping power increased by 104% in the wavy channel with a dimple at the channel throat</p> <p>Challenges and limitations:</p> <ul style="list-style-type: none">• The existence of concave dimple geometry in the cavity area reduced the fluid velocity and fluid mixing, thus increasing the thermal resistance• For design optimisation, a convex dimple should be considered in the design development. A convex dimple geometry in the cavity area will generate the jet effect and thus can increase the fluid velocity at the sidewalls of the cavity. This can enhance the heat transfer rate in the cavity area

Table 2: Continued

Xie et al. [101]	<p>Design: Flow disruption, re-entrant obstruction, and surface roughness methods</p>   <p>Overall performance: The range of Nusselt number and friction factor ratio were 1.45–26.19 and 0.86–110.18, respectively</p> <p>Challenges and limitations:</p> <ul style="list-style-type: none">• Nozzle effect provided by protrusions at the opposite surfaces increased the heat transfer performance because of high-velocity gradient generated close to the wall. However, the pressure drop issue restricted the overall performance of the designs. The pressure drop penalty can be minimised by optimising the parameter of rib geometry in a future study
Gong et al. [93]	<p>Design: Re-entrant obstruction and surface roughness methods</p>  <p>Overall performance: The PEC of the proposed design was about 1.33 at a Re of 200</p> <p>Challenges and limitations:</p> <ul style="list-style-type: none">• A new combination of a concave dimple geometry and two convex dimple geometries should be considered in a future study. The two convex dimple geometries behind the concave dimple geometry (at the channel's throat) can increase the fluid velocity of the mainstream in the cavity area which has a lower speed. The Nozzle effect by the concave dimple geometries can improve the convective heat transfer at the sidewalls of the cavity geometry
Xia et al. [99]	<p>Design: Flow disruption, re-entrant obstruction, and surface roughness methods</p>  <p>Overall performance: The highest Nusselt number and friction factor ratio were about 2.4 and 7, respectively, at a Re of 600</p> <p>Challenges and limitations:</p> <ul style="list-style-type: none">• The effect of distance between rib and cavity geometries can be analysed in future work. The nozzle effect generated by the rib geometry near the cavity area can reduce the residence time of fluid in the cavity area. Besides that, vortex flow induced by the rib geometry because of adverse pressure gradient can change the flow structure of fluid at the nearest cavity area, where the increase in the degree of flow mixing can contribute to the enhancement of heat transfer performance

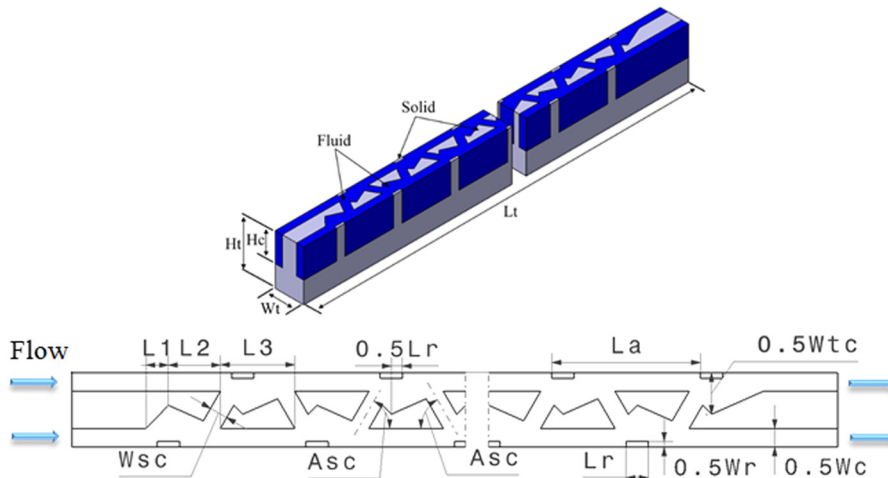


Figure 2: Hybrid MCHS with secondary channel geometry [111].

Some criteria need to be considered during the preparation of nanofluid, which include base fluid selection, size, shape, concentration, purity, dispersibility, thermal conductivity, preparation method (dispersion technique and sonication time [121,122]), and compatibility of nanoparticles that ensure the homogeneity of nanofluid [123]. Table 3 shows some types of nanoparticles that have been used in the MCHS application in the previous studies [124–136] such as an aluminium dioxide (Al_2O_3), multi-walled carbon nanotube (MWCNT), silicon dioxide (SiO_2), Titanium dioxide (TiO_2), silver (Ag), single-wall carbon nanotube (SWCNT), copper (Cu), copper oxide (CuO), zinc (Zn), silicon carbide (SiC), and iron(II,III) oxide (Fe_3O_4). It can be observed that most of the researchers were interested in Al_2O_3 nanoparticle as an additive in a base fluid for the MCHS application. Besides that, pure water such as deionised (DI) and distilled water was widely used as a base fluid in the analysis. Alfaryjat et al. [133] studied the effect of the base fluid type that was homogenised with Al_2O_3 nanoparticle on the fluid flow and heat transfer characteristics in a rhombus MCHS. They revealed that Al_2O_3 nanoparticle that was dispersed in pure water had the highest heat transfer coefficient compared to other base fluids such as engine oil, glycerine, and ethylene glycol (EG). Furthermore, Al_2O_3 in water provided the lowest thermal resistance among the other base fluids. Although all the base fluids have a similar friction factor, Al_2O_3 /water generated the smallest pressure drop that minimised the pumping power consumption compared to other base fluids. The findings were further supported by Lyu et al. [137] where water-based nanofluid provided higher cooling performance and lower pumping power consumption than kerosene-based nanofluid in a fractal

MCHS. For more understanding about the performance of Al_2O_3 nanoparticle as an additive, Thansekhar and Anbumeenakshi [128] analysed the effect of thermo-physical properties of nanoparticles on the heat transfer performance for a low Re of 55–90 experimentally. The Al_2O_3 /water resulted in a better heat transfer performance compared to SiO_2 /water because of the thermal conductivity of the former. Thermal conductivity is one of the factors that determine the performance of nanofluid.

However, Razali et al. [138] found that the performance of Al_2O_3 /water decreased when used for a longer period because of the changes in the crystallite size of Al_2O_3 that was affected by its growth during the heating process. To overcome the crystallisation problem upon heating, Sivakumar et al. [125] studied on another potential additive, CuO nanoparticle. The performance of Al_2O_3 nanoparticle was compared with CuO nanoparticle using different base fluids such as EG and pure water. The results showed that the heat transfer coefficient of CuO /EG was higher than Al_2O_3 /water and CuO /water that could be attributed to the higher viscosity and density of EG as the base fluid. However, the findings contradicted with that reported by Alfaryjat et al. [133] where water was found to perform better as a base fluid compared to EG. Besides the type of base fluid, the volume concentration of nanoparticle also affects the heat transfer performance negatively or positively. The most common volume concentration used in the previous studies was less than 2%. Chabi et al. [139] claimed that nanofluid with a high volume concentration tends to reduce the heat transfer coefficient because of the rapid formation of sedimentation besides reducing the nanofluid stability. The statement by Chabi et al. [139] was further supported

Table 3: Utilisation of nanofluids in the MCHS application with different nanoparticle concentration/diameter and flow condition

Reference	Re	Nanofluid	Volume concentration/ diameter	Base fluid	Findings
Arbappour et al. [135]	1–100	MWCNT	4% (v/v), 8% (v/v)	Kerosene	<p>Numerical work:</p> <ul style="list-style-type: none"> Thermal resistance decreased with increasing volume fraction and slip velocity coefficient Heat transfer increased with Re and volume concentration of nanoparticles Pressure drop increased with increasing nanoparticle volume fraction Increasing volume fraction increased the friction coefficient because of the enhancement of viscosity and density <p>Numerical work:</p> <ul style="list-style-type: none"> Thermal resistance was improved up to 6.7% when 1% TiO₂ (v/v) nanofluid was compared with base fluid The thermal resistance of 1% TiO₂ (v/v) nanofluid was lower than Al₂O₃ nanofluid at the same concentration Higher thermal performance was achieved with nanofluid that has a higher thermal conductivity and concentration <p>Experimental work:</p> <ul style="list-style-type: none"> The optimum concentration of 0.05% Ag nanofluid (w/v) enhanced the overall thermal performance by 37% at a Re of 1,400 0.1% Ag nanofluid (w/v) increased the heat transfer coefficient by 47% and found to be the highest Heat transfer coefficient and pressure drop increased with increasing mass concentration
Tran et al. [136]	100–900	Al ₂ O ₃ , TiO ₂	0.1% (v/v), 0.5% (v/v), 1.0% (v/v)	DI water	<p>Numerical work:</p> <ul style="list-style-type: none"> Al₂O₃/water resulted in the lowest thermal resistance and pumping power consumption in a rhombus shape cross-section Water-based fluid exhibited similar friction factor as base fluids analysed Al₂O₃/water had the highest heat transfer coefficient compared to Al₂O₃ nanoparticle with other base fluids evaluated <p>Numerical work:</p> <ul style="list-style-type: none"> There was no significant effect on pressure drop by nanofluid utilisation in the interrupted MCHS At least 2.0% (v/v) was required to enhance the heat transfer performance 5% of Al₂O₃/water (v/v) enhanced the Nusselt number by more than 30% and significantly impacted heat transfer performance
Sarafraz et al. [134]	50–1,400	Ag	0.01% (w/v), 0.05% (w/v), 0.10% (w/v)	DI water	<p>Numerical work:</p> <ul style="list-style-type: none"> Al₂O₃/water resulted in the lowest thermal resistance and pumping power consumption in a rhombus shape cross-section Water-based fluid exhibited similar friction factor as base fluids analysed Al₂O₃/water had the highest heat transfer coefficient compared to Al₂O₃ nanoparticle with other base fluids evaluated <p>Numerical work:</p> <ul style="list-style-type: none"> There was no significant effect on pressure drop by nanofluid utilisation in the interrupted MCHS At least 2.0% (v/v) was required to enhance the heat transfer performance 5% of Al₂O₃/water (v/v) enhanced the Nusselt number by more than 30% and significantly impacted heat transfer performance
Alfaryjat et al. [133]	700	Al ₂ O ₃	4% (v/v), 25 nm	DI water, engine oil, glycerine, EG	<p>Numerical work:</p> <ul style="list-style-type: none"> Al₂O₃/water resulted in the lowest thermal resistance and pumping power consumption in a rhombus shape cross-section Water-based fluid exhibited similar friction factor as base fluids analysed Al₂O₃/water had the highest heat transfer coefficient compared to Al₂O₃ nanoparticle with other base fluids evaluated <p>Numerical work:</p> <ul style="list-style-type: none"> There was no significant effect on pressure drop by nanofluid utilisation in the interrupted MCHS At least 2.0% (v/v) was required to enhance the heat transfer performance 5% of Al₂O₃/water (v/v) enhanced the Nusselt number by more than 30% and significantly impacted heat transfer performance
Abdollahi et al. [132]	200–700	Al ₂ O ₃	1.0% (v/v), 2.5% (v/v), 5.0% (v/v)	DI water	<p>Numerical work:</p> <ul style="list-style-type: none"> Al₂O₃/water resulted in the lowest thermal resistance and pumping power consumption in a rhombus shape cross-section Water-based fluid exhibited similar friction factor as base fluids analysed Al₂O₃/water had the highest heat transfer coefficient compared to Al₂O₃ nanoparticle with other base fluids evaluated <p>Numerical work:</p> <ul style="list-style-type: none"> There was no significant effect on pressure drop by nanofluid utilisation in the interrupted MCHS At least 2.0% (v/v) was required to enhance the heat transfer performance 5% of Al₂O₃/water (v/v) enhanced the Nusselt number by more than 30% and significantly impacted heat transfer performance

Table 3: Continued

Reference	Re	Nanofluid	Volume concentration/ diameter	Base fluid	Findings
Vinoth et al. [131]	300–850	Al ₂ O ₃	0.25% (v/v)	Distilled water	Experimental work: <ul style="list-style-type: none"> • By dispersing Al₂O₃ nanoparticle in the water, the heat transfer rate increased up to 4.6% • Heat transfer rate augmentation of the trapezoidal cross-section of oblique finned MCHS was the highest compared to square and semi-circle cross-section for both water and nanofluid by 3.13 and 5.88%, respectively
Duangthongsuk et al. [130]	NA	SiO ₂	0.3% (v/v), 0.6% (v/v), 0.8% (v/v)	DI water	Experimental work: <ul style="list-style-type: none"> • Thermal performance improvement by nanofluid was better than water by 3–15% • The utilisation of nanofluid in cross-cutting flow channel resulted in a small increment in pressure drop • Nusselt number increased with increasing volume concentration and Re
Arani et al. [129]	500–2,000	SWCNT	4% (v/v), 8% (v/v)	Distilled water	Numerical work: <ul style="list-style-type: none"> • Thermal resistance, the ratio of maximum temperature to minimum temperature on the bottom surface, and the ratio of thermal resistance decreased with increasing volume fraction and Re • Heat transfer rate increased with increasing volume fraction • Pressure drop increased with increasing volume fraction
Thansekhar and Anbumeenakshi [128]	55–90	Al ₂ O ₃ , SiO ₂	0.1% (v/v), 0.25% (v/v)	DI water	Experimental work: <ul style="list-style-type: none"> • Al₂O₃/water showed a better heat transfer performance than SiO₂/water because of the thermal conductivity Al₂O₃/water • Heat transfer increased with increasing volume fraction that was attributed to stronger thermal dispersion and thermophoresis • The presence of nanofluid at a low Re in the rectangular microchannel has a smaller effect on pressure drop
Sarafraz et al. [127]	100–1,400	MWCNT	0.05% (w/v), 0.1% (w/v), 0.45% (w/v)	DI water	Experimental work: <ul style="list-style-type: none"> • MWCNT had a higher heat transfer coefficient than the other base fluids. Approximately 29% enhancement of the heat transfer coefficient was recorded • Heat transfer increased significantly with increasing nanofluid volume concentration and fluid flow rate • Constant fouling thermal resistance was achieved at a lower operating time for the higher mass concentration

Table 3: Continued

Reference	Re	Nanofluid	Volume concentration/ diameter	Base fluid	Findings
Snoussi et al. [126]	100–1,000	Al ₂ O ₃ Cu	1.0% (v/v), 2.0% (v/v)	DI water	<ul style="list-style-type: none"> MWCNT provided lower temperature profile in MCHS for the higher mass concentration <p>Numerical work:</p> <ul style="list-style-type: none"> Nanofluid was most effective when a higher heat flux was applied At a higher heat flux, wall temperature decreased with increasing volume fraction Heat transfer performance increased by 14–20% when nanofluid was used
Abubakar et al. [124]	140, 700, 1,400	Fe ₃ O ₄	0.4% (v/v), 0.6% (v/v), 0.8% (v/v)	Distilled water	<p>Numerical work:</p> <ul style="list-style-type: none"> The presence of Fe₃O₄ nanoparticle in pure water resulted in a better heat transfer performance than pure water only because of the higher dynamic viscosity and lower heat capacity of the nanoparticle The temperature of the channel wall decreased with the increasing volume fraction of Fe₃O₄ When Fe₃O₄/water was used, the surface temperature decreased by 0.04, 0.07, and 0.08% for 0.4, 0.6, and 0.8% of concentrations, respectively
Sivakumar et al. [125]	100–1,300	CuO, Al ₂ O ₃	NA	EG, Distilled water	<p>Experimental and numerical work:</p> <ul style="list-style-type: none"> Heat transfer coefficients for CuO/EG and Al₂O₃/water were higher than that of base fluids Heat transfer coefficient of CuO/EG was higher than that of Al₂O₃/water and CuO/water Brownian motion of nanoparticle in serpentine shape channel enhanced the heat transfer rate

by Manay and Sahin [140] where a volume concentration of less than 2.0% of TiO_2 nanoparticle increased the overall thermal efficiency with an increasing volume concentration of nanoparticle. However, at a higher volume concentration, the heat transfer performance decreased. Increasing the volume concentration also significantly affected the thermal resistance because of particle deposition. Furthermore, the reduction in thermal resistance was reported when nanoparticle of an average diameter of 25 nm was used.

All studies reviewed in this paper supported the fact that nanoparticles that dispersed in a base fluid can enhance the heat transfer performance in an MCHS. However, at a higher volume concentration of nanofluid, high-pressure drop penalty dominated the thermal performance enhancement. Majority of studies focused on the use of water as the base fluid and Al_2O_3 nanoparticle as the additive. According to Elsevier database from 2015 to 2017, 87% of the published papers used water (DI water or distilled water) as a base fluid for nanofluid preparation in MCHS application as shown in Figure 3. Besides that, higher application of Al_2O_3 nanoparticle as additives in an MCHS was noted compared to the use of MWCNT, TiO_2 , Ag, SiO_2 , SWCNT, Cu, CuO, Zn, and SiC as additives as illustrated in Figure 4. Nanofluid concentration was found to significantly affect the overall performance of an MCHS. The use of optimum nanofluid concentration helps to minimise the penalty of pressure drop in an MCHS. Figure 5 presents the concentration of nanofluid, which was commonly used in the MCHS application. Most of the studies used nanoparticle dispersed in a base fluid with maximum concentrations of 2% (v/v) for the MCHS application.

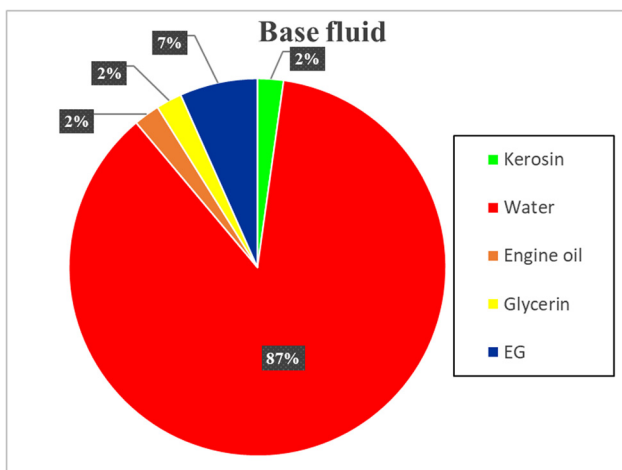


Figure 3: Type of base fluids commonly used in nanofluid preparation.

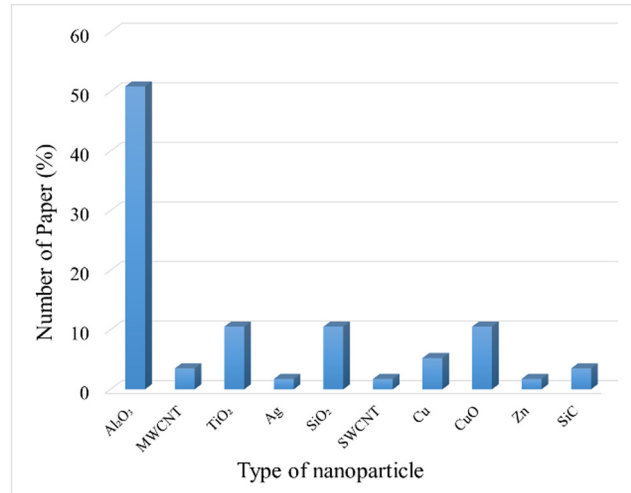


Figure 4: Type of nanoparticles commonly used in nanofluid preparation.

3 Future prospects of MCHS with passive method and Moore's Law

Rapid development of MCHS in the thermal management of electronic device is expected to be continued until the year of 2040. According to Moore's law used by Intel for transistor count observation, the number of transistors has doubled every 24 months [141–145] as shown in Figure 6 [142]. There are three measures considered in the increasing number of transistors per microchips, such as shrinking the size of the single transistor (scaling), increasing the microchip area, and improving circuit and device design. As we can see here, scaling down the individual transistor and microchip size in

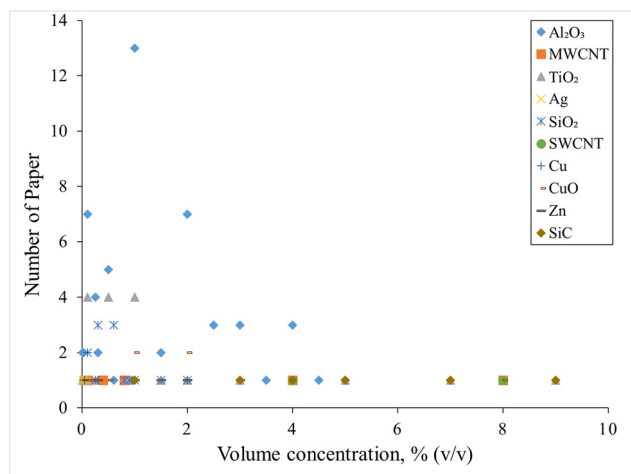


Figure 5: Distribution of nanoparticle concentration commonly used in MCHS applications.

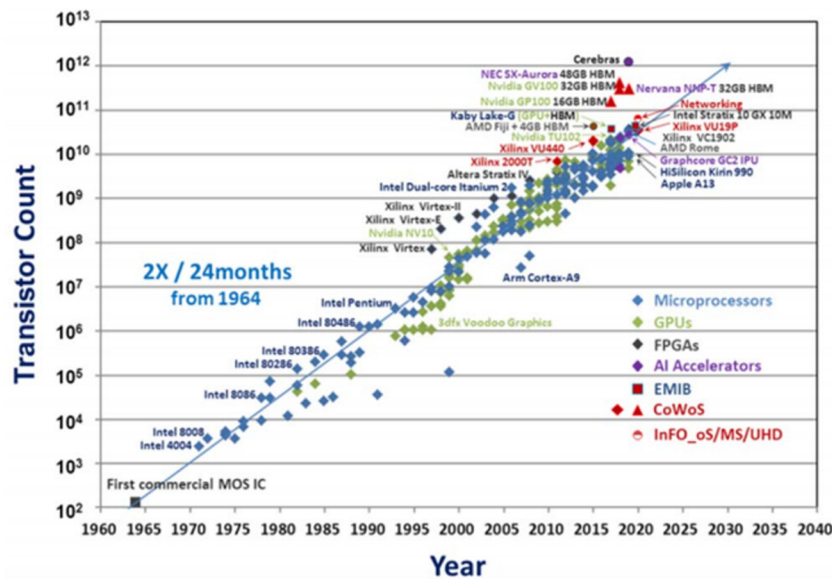


Figure 6: Evolution of transistor count according to Moore's law [142].

improving the microprocessor performance (as shown in Figure 7) [146,147] has caused detrimental effects leading to high heat dissipation. This is one of the biggest challenges in the microchip development [148]. As a consequence, urgent needs for the advanced cooling device are rising by years.

In recent years, the microchip development has saturated because the size of 3D transistor reached its physical limit because of the scaling down effect. In 2019, Li et al. [149] proposed a 2D transistor, which enabled to

extend the Moore's law, to replace the 3D transistor that can shrink further. Therefore, heat will dissipate exponentially in the future.

As mentioned in the previous section, a microchannel is a spin-off technology that can be implemented in many fields. Why microchannel becomes the first choice compared to nanochannel in many application? This is because microchannel can be fabricated by micro-machining process with the high-quality output. In contrast, nanochannel is fabricated by laser machining process with some issues output such as cracking, ripple formation, shape deformation, and debris deposition [150,151].

MCHS has a bright future in many applications. Based on the market research report [152], MCHS is one of the cooling technologies that expected to grow at the highest compound annual growth rate (CAGR) in the global thermal management market for the global forecast of the year 2025.

4 Conclusion

Current designs of MCHSs with novel channel designs that could result in a high heat transfer rate with acceptable pressure drop penalty were comprehensively reviewed in this study. This review is expected to provide a better understanding of microchannel design development and the effects of geometry design on hydrothermal performances such as heat transfer and fluid flow characteristics.

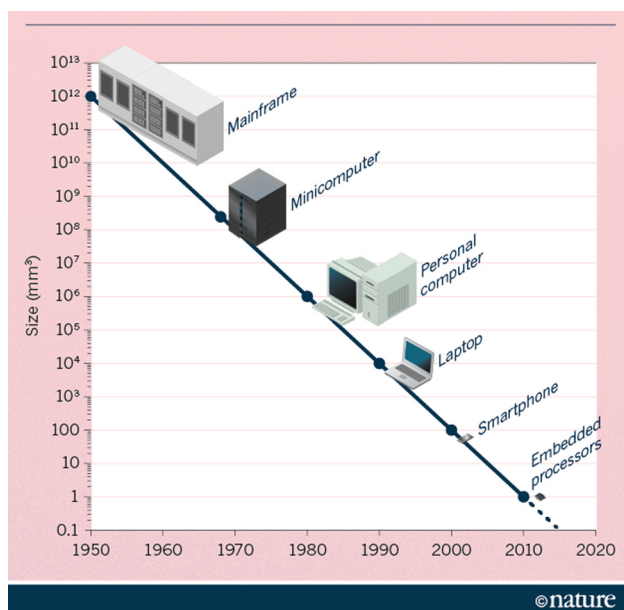


Figure 7: Evolution of microchip size [146,147].

These two characteristics are critical in the design development of MCHS to achieve high heat transfer rate with a low cost concerning energy consumption. Besides that, the effect of widely used nanoparticle concentration, type, and base fluid selection on nanofluid performance and stability in the MCHS application have been discussed and summarised. Following are the main conclusions that can be derived from this review:

- (a) Hydraulic performance of hybrid passive method of MCHS was better than single passive method of MCHS over a wide range of Re. Rapid development of vortices flow formation at low Re increases fluid mixing in the hybrid MCHS with low pressure drop penalty, and thus reduces pumping power consumption.
- (b) Combination of more than one passive method in a hybrid MCHS can achieve a high heat transfer performance with minimal pressure drop penalty. However, sometimes the minimal pressure drop penalty can be very high because of the friction factor influenced by geometry structure. Therefore, the optimum hydrothermal performance should also consider the friction factor to prevent any leakage in the pipelines or channels.
- (c) The key strategy to improve the heat transfer performance is to increase the fluid mixing and redevelop the boundary layer in the laminar flow, which can be achieved by changing the flow profile. The out-of-flow mixing method is the best method that can provide a high degree of flow mixing; however, this method results in a high-pressure drop. Alternatively, the secondary flow generated by secondary channel geometry can be very useful to increase the degree of flow mixing without a high-pressure drop.
- (d) The surface roughness method is the best method to reduce friction factor and at the same time can enhance the heat transfer rate by providing a larger heat transfer area. However, this method is ineffective if applied as a single method, as the recirculation zone in the cavity area causes the fluid to remain in the cavity and does not remove the heat flux efficiently. By combining the method with flow disruption method, the fluid in the cavity area can be replaced easily by guiding the mainstream at the centre channel to the cavity area using the rib geometry.
- (e) The physical properties of base fluid such as thermal conductivity, dynamic viscosity, heat capacity, and density significantly affected the nanofluid performance. Pure water such as DI water and distilled water were widely used as the base fluid for nanofluid preparation for the MCHS application.

- (f) Each nanoparticle has a limited range of volume concentration utilisation. Optimum volume concentration application can increase the heat transfer performance with a minimal pressure drop in the MCHS application. However, higher nanoparticle volume concentration in a base fluid can increase the thermal resistance because of particle deposition and thus reducing the overall thermal performance of the MCHS. Nanoparticle solution with a volume concentration of less than 2% is suggested. Besides, Al_2O_3 nanoparticle is recommended to be used as an additive, which is commonly used in MCHS applications for nanofluid preparation.

Acknowledgments: The authors would like to thank Malaysia-Japan International Institute of Technology (MJIIT) and Universiti Teknologi Malaysia for supporting this research. This work was funded by the FRGS-MSRA grant [R.K130000.7843.5F273], LRGS grant [R.K130000.7843.4L891], and TAKASAGO grant [R.K130000.7343.4B472].

Conflict of interest: The authors declare no conflicts of interest regarding the publication of this paper.

References

- [1] Sidik NAC, Muhamad, MNAW, Japar WMAA, Rasid ZA. An overview of passive techniques for heat transfer augmentation in microchannel heat sink. *Int Commun Heat Mass Transf.* 2017;88:74–83.
- [2] Black JR. Electromigration – A brief survey and some recent results. *IEEE Trans Electron Devices.* 1969;16(4):338–47.
- [3] Farsad E, Abbasi S, Zabihi M, Sabbaghzadeh J. Numerical simulation of heat transfer in a micro channel heat sinks using nanofluids. *Heat Mass Transf.* 2011;47(4):479–90.
- [4] Ghani IA, Sidik NAC, Kamaruzaman N. Hydrothermal performance of microchannel heat sink: The effect of channel design. *Int J Heat Mass Transf.* 2017;107:21–44.
- [5] Dugan JF, Anderson SD. Electronic device fan mounting system. Google Pat. no: 6,244,953; 2001.
- [6] Chang Y-W, Cheng C-H, Wang J-C, Chen S-L. Heat pipe for cooling of electronic equipment. *Energy Convers Manage.* 2008;49(11):3398–404.
- [7] Deng Y, Liu J. A liquid metal cooling system for the thermal management of high power LEDs. *Int Commun Heat Mass Transf.* 2010;37(7):788–91.
- [8] Gong L, Zhao J, Huang S. Numerical study on layout of micro-channel heat sink for thermal management of electronic devices. *Appl Therm Eng.* 2015;88:480–90.
- [9] Lee J-H. Micro cooling device. Google Pat. no: 6,698,502 2004.

- [10] Single-phase heat transfer enhancement techniques in microchannel and minichannel flows. In: Steinke ME, Kandlikar SG, editors. ASME 2004 2nd international conference on microchannels and minichannels; 2004.
- [11] Noh N, Fazeli A, Sidik NC. Numerical simulation of nanofluids for cooling efficiency in microchannel heat sink. *J Adv Res Fluid Mech Therm Sci.* 2014;4(1):13–23.
- [12] Tuckerman DB, Pease RFW. High-performance heat sinking for VLSI. *IEEE Electron Device Lett.* 1981;2(5):126–9.
- [13] Japar WMAA, Sidik NAC, Kamaruzaman N, Asako Y, Muhammad NMA. Hydrothermal performance in the hydrodynamic entrance region of rectangular microchannel heat sink. *J Adv Res Numer Heat Transf.* 2020;1(1):22–31.
- [14] Optimization of microchannel heat sinks using entropy generation minimization method. In: Khan WA, Yovanovich M, Culham J, editors. Twenty-second annual IEEE semiconductor thermal measurement and management symposium. IEEE; 2006.
- [15] Optimization of heat transfer rate in the rectangular microchannel of different aspect ratios with constant cross sectional area. In: Kowsari F, Noroozi N, Rezaei Barmi M, editors. ASME 2008 first international conference on micro/nano-scale heat transfer; 2008.
- [16] Microchannel optimization for heat dissipation from a solid substrate. In: Sobhan CB, Anoop PS, Arimboor K, Abraham T, Peterson GP, editors. ASME 2008 first international conference on micro/nanoscale heat transfer; 2008.
- [17] Kou H-S, Lee J-J, Chen C-W. Optimum thermal performance of microchannel heat sink by adjusting channel width and height. *Int Commun Heat Mass Transf.* 2008;35(5):577–82.
- [18] Chong S, Ooi K, Wong T. Optimisation of single and double layer counter flow microchannel heat sinks. *Appl Therm Eng.* 2002;22(14):1569–85.
- [19] Wei X, Joshi Y. Optimization study of stacked micro-channel heat sinks for micro-electronic cooling. *IEEE Trans Compon Packag Technol.* 2003;26(1):55–61.
- [20] Hung T-C, Yan W-M. Optimization of a microchannel heat sink with varying channel heights and widths. *Numer Heat Transfer, Part A: Appl.* 2012;62(9):722–41.
- [21] Wang T-H, Wu H-C, Meng J-H, Yan W-M. Optimization of a double-layered microchannel heat sink with semi-porous ribs by multi-objective genetic algorithm. *Int J Heat Mass Transf.* 2020;149:119217.
- [22] Pantic S, Skodric SR, Loncar Z, Pantic I. Zinc oxide nanoparticles: Potential novel applications in cellular physiology, pathology, neurosciences and cancer research. *Rev Adv Mater Sci.* 2019;58(1):17–21.
- [23] Huang D, Wu K, Zhang Y, Ni Z, Zhu X, Zhu C, et al. Recent advances in tissue plasminogen activator-based nanothrombolysis for ischemic stroke. *Rev Adv Mater Sci.* 2019;58(1):159–70.
- [24] Pantic S, Skodric SR, Loncar Z, Pantic I. Neurotoxicity, nephrotoxicity, and hepatotoxicity of copper-based nanoparticles: Potential implications in molecular medicine and neurosciences. *Rev Adv Mater Sci.* 2019;58(1):201–5.
- [25] Godlewski MM, Kaszewski J, Kielbik P, Olszewski J, Lipinski W, Slonska-Zielonka A, et al. New generation of oxide-based nanoparticles for the applications in early cancer detection and diagnostics. *Nanotechnol Rev.* 2020;9(1):274–302.
- [26] Li J, Yao M, Shao Y, Yao D. The application of bio-nanotechnology in tumor diagnosis and treatment: A view. *Nanotechnol Rev.* 2018;7(3):257–66.
- [27] Yao L, Xu S. Detection of magnetic nanomaterials in molecular imaging and diagnosis applications. *Nanotechnol Rev.* 2014;3(3):247–68.
- [28] Ban I, Stergar J, Maver U. NiCu magnetic nanoparticles: Review of synthesis methods, surface functionalization approaches, and biomedical applications. *Nanotechnol Rev.* 2018;7(2):187–207.
- [29] Dürr S, Janko C, Lyer S, Tripal P, Schwarz M, Zaloga J, et al. Magnetic nanoparticles for cancer therapy. *Nanotechnol Rev.* 2013;2(4):395–409.
- [30] Manohar CS, Kumar BS, Sadhu SPP, Srimadh SK, Muthukumar VS, Venketesh S, et al. Novel lead-free bio-compatible piezoelectric hydroxyapatite (HA)–BCZT ($\text{Ba}_{0.85}\text{Ca}_{0.15}\text{Zr}_{0.1}\text{Ti}_{0.9}\text{O}_3$) nanocrystal composites for bone regeneration. *Nanotechnol Rev.* 2019;8(1):61–78.
- [31] Yousefi AM, Oudadesse H, Akbarzadeh R, Wers E, Lucas-Girot A. Physical and biological characteristics of nanohydroxyapatite and bioactive glasses used for bone tissue engineering. *Nanotechnol Rev.* 2014;3(6):527–52.
- [32] Sarker B, Lyer S, Arkudas A, Boccaccini AR. Collagen/silica nanocomposites and hybrids for bone tissue engineering. *Nanotechnol Rev.* 2013;2(4):427–47.
- [33] Guo S, Fu D, Utupova A, Sun D, Zhou M, Jin Z, et al. Applications of polymer-based nanoparticles in vaccine field. *Nanotechnol Rev.* 2019;8(1):143–55.
- [34] Otto DP, De Villiers MM. Why is the nanoscale special (or not)? Fundamental properties and how it relates to the design of nano-enabled drug delivery systems. *Nanotechnol Rev.* 2013;2(2):171–99.
- [35] Sawicki K, Czajka M, Matysiak-Kucharek M, Fal B, Drop B, Męczyńska-Wielgosz S, et al. Toxicity of metallic nanoparticles in the central nervous system. *Nanotechnol Rev.* 2019;8(1):175–200.
- [36] Jia F, Li G, Yang B, Yu B, Shen Y, Cong H. Investigation of rare earth upconversion fluorescent nanoparticles in biomedical field. *Nanotechnol Rev.* 2019;8(1):1–17.
- [37] Puthenveetil R, Nguyen K, Vinogradova O. Nanodiscs and solution NMR: Preparation, application and challenges. *Nanotechnol Rev.* 2017;6(1):111–25.
- [38] Mineev KS, Nadezhdin KD. Membrane mimetics for solution NMR studies of membrane proteins. *Nanotechnol Rev.* 2017;6(1):15–32.
- [39] Xu J, Yang B. Nanostructured phase-changeable heat transfer fluids. *Nanotechnol Rev.* 2013;2(3):289–306.
- [40] Beng SW, Japar WMAA. Numerical analysis of heat and fluid flow in microchannel heat sink with triangular cavities. *J Adv Res Fluid Mech Therm Sci.* 2017;34(1):1–8.
- [41] Adham AM, Mohd-Ghazali N, Ahmad R. Thermal and hydrodynamic analysis of microchannel heat sinks: A review. *Renew Sustain Energy Rev.* 2013;21:614–22.
- [42] Kumar S, Kumar A, Kothiyal AD, Bisht MS. A review of flow and heat transfer behaviour of nanofluids in micro channel heat sinks. *Therm Sci Eng Prog.* 2018;8:477–93.
- [43] Go JS. Design of a microfin array heat sink using flow-induced vibration to enhance the heat transfer in the laminar flow regime. *Sens Actuators, A.* 2003;105(2):201–10.

- [44] Yeom T, Simon TW, Huang L, North MT, Cui T. Piezoelectric translational agitation for enhancing forced-convection channel-flow heat transfer. *Int J Heat Mass Transf.* 2012;55(25–26):7398–409.
- [45] Yeom T, Simon T, Zhang M, Yu Y, Cui T. Active heat sink with piezoelectric translational agitators, piezoelectric synthetic jets, and micro pin fin arrays. *Exp Therm Fluid Sci.* 2018;99:190–9.
- [46] Krishnaveni T, Renganathan T, Picardo J, Pushpavanam S. Numerical study of enhanced mixing in pressure-driven flows in microchannels using a spatially periodic electric field. *Phys Rev E.* 2017;96(3):033117.
- [47] Heat transfer enhancement in an electrically heated horizontal pipe due to flow pulsation. In: Hessami M-A, Berryman A, Bandopdhayay P, editors. *ASME 2003 international mechanical engineering congress and exposition*; 2003.
- [48] Zhang H, Li S, Cheng J, Zheng Z, Li X, Li F. Numerical study on the pulsating effect on heat transfer performance of pseudo-plastic fluid flow in a manifold microchannel heat sink. *Appl Therm Eng.* 2018;129:1092–105.
- [49] Wang C-S, Wei T-C, Shen P-Y, Liou T-M. Lattice Boltzmann study of flow pulsation on heat transfer augmentation in a louvered microchannel heat sink. *Int J Heat Mass Transf.* 2020;148:119139.
- [50] Shen S, Xu J, Zhou J, Chen Y. Flow and heat transfer in microchannels with rough wall surface. *Energy Convers Manage.* 2006;47(11–12):1311–25.
- [51] Jones BJ, Garimella SV. Surface roughness effects on flow boiling in microchannels. *J Therm Sci Eng Appl.* 2009;1(4):041007.
- [52] Gulbe L, Jekabsons N, Traskovs A. Parametric studies for vertical axis wind turbine simulations. *Environ Clim Technol.* 2011;6(1):23–30.
- [53] Alam T, Lee PS, Yap CR. Effects of surface roughness on flow boiling in silicon microgap heat sinks. *Int J Heat Mass Transf.* 2013;64:28–41.
- [54] Ma T. Effects of surface roughness on thermal and hydrodynamic behaviors in microchannel using lattice Boltzmann method. *Int J Fluid Machinery Syst.* 2017;10(4):439–46.
- [55] Javanbakht M-H, Moosavi A. Heat transfer on topographically structured surfaces for power law fluids. *Int J Heat Mass Transf.* 2018;121:857–71.
- [56] Jing D, Song S, Pan Y, Wang X. Size dependences of hydraulic resistance and heat transfer of fluid flow in elliptical microchannel heat sinks with boundary slip. *Int J Heat Mass Transf.* 2018;119:647–53.
- [57] Hong F, Cheng P. Three dimensional numerical analyses and optimization of offset strip-fin microchannel heat sinks. *Int Commun Heat Mass Transf.* 2009;36(7):651–6.
- [58] Chai L, Xia G, Zhou M, Li J, Qi J. Optimum thermal design of interrupted microchannel heat sink with rectangular ribs in the transverse microchambers. *Appl Therm Eng.* 2013;51(1–2):880–9.
- [59] Xie G, Zhang F, Sundén B, Zhang W. Constructal design and thermal analysis of microchannel heat sinks with multistage bifurcations in single-phase liquid flow. *Appl Therm Eng.* 2014;62(2):791–802.
- [60] Kamal H, Dewan A. Analysis of interrupted rectangular microchannel heat sink with high aspect ratio. *J Appl Fluid Mech.* 2017;10(1):117–26.
- [61] Chai L, Wang L. Thermal-hydraulic performance of interrupted microchannel heat sinks with different rib geometries in transverse microchambers. *Int J Therm Sci.* 2018;127:201–12.
- [62] Mario Di Capua H, Escobar R, Diaz A, Guzmán AM. Enhancement of the cooling capability of a high concentration photovoltaic system using microchannels with forward triangular ribs on sidewalls. *Appl Energy.* 2018;226:160–80.
- [63] Saravanan V, Umesh C. Numerical comparison for thermo-hydraulic performance of pin fin heat sink with micro channel pin fin heat sink. *Sādhana.* 2018;43(7):100.
- [64] Shen H, Liu X, Yan H, Xie G, Sundén B. Enhanced thermal performance of internal y-shaped bifurcation microchannel heat sinks with metal foams. *J Therm Sci Eng Appl.* 2018;10(1):011001.
- [65] Shen H, Wang C-C, Xie G. A parametric study on thermal performance of microchannel heat sinks with internally vertical bifurcations in laminar liquid flow. *Int J Heat Mass Transf.* 2018;117:487–97.
- [66] Sui Y, Teo C, Lee PS, Chew Y, Shu C. Fluid flow and heat transfer in wavy microchannels. *Int J Heat Mass Transf.* 2010;53(13–14):2760–72.
- [67] Mills ZG, Warey A, Alexeev A. Heat transfer enhancement and thermal-hydraulic performance in laminar flows through asymmetric wavy walled channels. *Int J Heat Mass Transf.* 2016;97:450–60.
- [68] Lin L, Zhao J, Lu G, Wang X-D, Yan W-M. Heat transfer enhancement in microchannel heat sink by wavy channel with changing wavelength/amplitude. *Int J Therm Sci.* 2017;118:423–34.
- [69] Hasis FBA, Krishna PM, Aravind G, Deepu M, Shine S. Thermo hydraulic performance analysis of twisted sinusoidal wavy microchannels. *Int J Therm Sci.* 2018;128:124–36.
- [70] Parlak Z. Optimal design of wavy microchannel and comparison of heat transfer characteristics with zigzag and straight geometries. *Heat Mass Transf.* 2018;54(11):3317–28.
- [71] Ermagan H, Rafee R. Numerical investigation into the thermo-fluid performance of wavy microchannels with superhydrophobic walls. *Int J Therm Sci.* 2018;132:578–88.
- [72] Navin Raja K. Thermal enhancement in a microchannel heat sink using passive methods/Navin Raja Kuppasamy. Kuala Lumpur, Malaysia: University of Malaya; 2016.
- [73] Deng D, Xie Y, Huang Q, Wan W. On the flow boiling enhancement in interconnected reentrant microchannels. *Int J Heat Mass Transf.* 2017;108:453–67.
- [74] Lee YJ, Lee PS, Chou SK. Enhanced thermal transport in microchannel using oblique fins. *J Heat Transf.* 2012;134(10):101901.
- [75] Kuppasamy NR, Saidur R, Ghazali N, Mohammed H. Numerical study of thermal enhancement in micro channel heat sink with secondary flow. *Int J Heat Mass Transf.* 2014;78:216–23.
- [76] Law M, Lee P-S, Balasubramanian K. Experimental investigation of flow boiling heat transfer in novel oblique-finned microchannels. *Int J Heat Mass Transf.* 2014;76:419–31.
- [77] Lee YJ, Singh PK, Lee PS. Fluid flow and heat transfer investigations on enhanced microchannel heat sink using oblique fins with parametric study. *Int J Heat Mass Transf.* 2015;81:325–36.

- [78] Law M, Lee P-S. A comparative study of experimental flow boiling heat transfer and pressure characteristics in straight- and oblique-finned microchannels. *Int J Heat Mass Transf.* 2015;85:797–810.
- [79] Law M, Kanargi OB, Lee P-S. Effects of varying oblique angles on flow boiling heat transfer and pressure characteristics in oblique-finned microchannels. *Int J Heat Mass Transf.* 2016;100:646–60.
- [80] Law M, Lee P-S. Effects of varying secondary channel widths on flow boiling heat transfer and pressure characteristics in oblique-finned microchannels. *Int J Heat Mass Transf.* 2016;101:313–26.
- [81] Viktorov V, Mahmud MR, Visconte C. Design and characterization of a new HC passive micromixer up to Reynolds number 100. *Chem Eng Res Des.* 2016;108:152–63.
- [82] Sivashankar S, Agambayev S, Mashraei Y, Li EQ, Thoroddsen ST, Salama KN. A “twisted” microfluidic mixer suitable for a wide range of flow rate applications. *Biomicrofluidics.* 2016;10(3):034120.
- [83] Huanming X, Jiawei W, Zhiping W. A comparative discussion of different designs of passive micromixers: Specific sensitivities of mixing efficiency on Reynolds numbers and fluid properties. *Microsyst Technol.* 2018;24(2): 1253–63.
- [84] Hayashi Y, Saneie N, Yip G, Kim YJ, Kim J-H. Metallic nanoe-mulsion with galinstan for high heat-flux thermal management. *Int J Heat Mass Transf.* 2016;101:1204–16.
- [85] Xia G, Liu R, Wang J, Du M. The characteristics of convective heat transfer in microchannel heat sinks using Al_2O_3 and TiO_2 nanofluids. *Int Commun Heat Mass Transf.* 2016;76:256–64.
- [86] Wu J, Zhao J, Lei J, Liu B. Effectiveness of nanofluid on improving the performance of microchannel heat sink. *Appl Therm Eng.* 2016;101:402–12.
- [87] Rabby MI, Masuri SU, Kaniappan L, Loulou T, Sadrul A. Effect of water based nanofluids on laminar convective heat transfer in developing region of rectangular channel. *CFD Lett.* 2019;11(12):74–87.
- [88] Japar WMAA, Sidik NAC, Saidur R, Asako Y, Mohd MI. Temperature minimization on the substrate of a heat sink by Rib-Groove microchannel heat sink with effective energy consumption: Groove geometry parameter effects. *CFD Lett.* 2019;11(9):1–13.
- [89] Bhandari P, Prajapati YK. Thermal performance of open microchannel heat sink with variable pin fin height. *Int J Therm Sci.* 2021;159:106609.
- [90] Yuan D, Zhou W, Fu T, Liu C. Experimental and numerical investigation of heat and mass transfer in non-uniform wavy microchannels. *Int J Therm Sci.* 2020;152:106320.
- [91] van Erp R, Soleimanzadeh R, Nela L, Kampitsis G, Matioli E. Co-designing electronics with microfluidics for more sustainable cooling. *Nature.* 2020;585(7824):211–6.
- [92] Li P, Luo Y, Zhang D, Xie Y. Flow and heat transfer characteristics and optimization study on the water-cooled micro-channel heat sinks with dimple and pin-fin. *Int J Heat Mass Transf.* 2018;119:152–62.
- [93] The characteristics of fluid flow and heat transfer in wavy, dimple and wavy-dimple microchannels. In: Gong L, Wei B, editors. *Applied Mechanics and Materials.* Switzerland: Trans Tech Publ; 2013.
- [94] Gong L, Lu H, Li H, Xu M. Parametric numerical study of the flow and heat transfer in a dimpled wavy microchannel. *Heat Transf Res.* 2016;47(2):105–18.
- [95] Srivastava P, Dewan A, Bajpai JK. Flow and heat transfer characteristics in convergent-divergent shaped micro-channel with ribs and cavities. *Int J Heat Technol.* 2017;35(4):863–73.
- [96] Li Y, Xia G, Ma D, Jia Y, Wang J. Characteristics of laminar flow and heat transfer in microchannel heat sink with triangular cavities and rectangular ribs. *Int J Heat Mass Transf.* 2016;98:17–28.
- [97] Li Y, Xia G, Jia Y, Ma D, Cai B, Wang J. Effect of geometric configuration on the laminar flow and heat transfer in microchannel heat sinks with cavities and fins. *Numer Heat Transfer, Part A: Appl.* 2017;71(5):528–46.
- [98] Ghani IA, Kamaruzaman N, Sidik NAC. Heat transfer augmentation in a microchannel heat sink with sinusoidal cavities and rectangular ribs. *Int J Heat Mass Transf.* 2017;108:1969–81.
- [99] Xia G, Zhai Y, Cui Z. Characteristics of entropy generation and heat transfer in a microchannel with fan-shaped reentrant cavities and internal ribs. *Sci China Technol Sci.* 2013;56(7):1629–35.
- [100] Xia G, Jia Y, Li Y, Ma D, Cai B. Numerical simulation and multiobjective optimization of a microchannel heat sink with arc-shaped grooves and ribs. *Numer Heat Transfer, Part A: Appl.* 2016;70(9):1041–55.
- [101] Xie Y, Shen Z, Zhang D, Lan J. Thermal performance of a water-cooled microchannel heat sink with grooves and obstacles. *J Electron Packag.* 2014;136(2):021001.
- [102] Ghani IA, Sidik NAC, Mamat R, Najafi G, Ken TL, Asako Y, et al. Heat transfer enhancement in microchannel heat sink using hybrid technique of ribs and secondary channels. *Int J Heat Mass Transf.* 2017;114:640–55.
- [103] Huang X, Yang W, Ming T, Shen W, Yu X. Heat transfer enhancement on a microchannel heat sink with impinging jets and dimples. *Int J Heat Mass Transf.* 2017;112:113–24.
- [104] Ming T, Cai C, Yang W, Shen W, Gan T. Optimization of dimples in microchannel heat sink with impinging jets – part A: Mathematical model and the influence of dimple radius. *J Therm Sci.* 2018;27(3):195–202.
- [105] Ming T, Cai C, Yang W, Shen W, Feng W, Zhou N. Optimization of dimples in microchannel heat sink with impinging jets – part B: The influences of dimple height and arrangement. *J Therm Sci.* 2018;27(4):321–30.
- [106] Yan Y, Yan H, Yin S, Zhang L, Li L. Single/multi-objective optimizations on hydraulic and thermal management in micro-channel heat sink with bionic Y-shaped fractal network by genetic algorithm coupled with numerical simulation. *Int J Heat Mass Transf.* 2019;129:468–79.
- [107] Bahiraei M, Jamshidmofid M, Goodarzi M. Efficacy of a hybrid nanofluid in a new microchannel heat sink equipped with both secondary channels and ribs. *J Mol Liq.* 2019;273:88–98.
- [108] Naqiuddin NH, Saw LH, Yew MC, Yusof F, Poon HM, Cai Z, et al. Numerical investigation for optimizing segmented micro-channel heat sink by Taguchi–Grey method. *Appl Energy.* 2018;222:437–50.
- [109] Wang R-J, Wang J-W, Lijin B-Q, Zhu Z-F. Parameterization investigation on the microchannel heat sink with slant

- rectangular ribs by numerical simulation. *Appl Therm Eng.* 2018;133:428–38.
- [110] Ansari D, Kim K-Y. Hotspot thermal management using a microchannel-pinfin hybrid heat sink. *Int J Therm Sci.* 2018;134:27–39.
- [111] Japar WMAA, Sidik NAC, Mat S. A comprehensive study on heat transfer enhancement in microchannel heat sink with secondary channel. *Int Commun Heat Mass Transf.* 2018;99:62–81.
- [112] Xie G, Li Y, Zhang F, Sundén B. Analysis of micro-channel heat sinks with rectangular-shaped flow obstructions. *Numer Heat Transfer, Part A: Appl.* 2016;69(4):335–51.
- [113] Lu H, Xu M, Gong L, Duan X, Chai JC. Effects of surface roughness in microchannel with passive heat transfer enhancement structures. *Int J Heat Mass Transf.* 2020;148:119070.
- [114] Yang M, Li M-T, Hua Y-C, Wang W, Cao B-Y. Experimental study on single-phase hybrid microchannel cooling using HFE-7100 for liquid-cooled chips. *Int J Heat Mass Transf.* 2020;160:120230.
- [115] Li Y, Wang Z, Yang J, Liu H. Thermal and hydraulic characteristics of microchannel heat sinks with cavities and fins based on field synergy and thermodynamic analysis. *Appl Therm Eng.* 2020;175:115348.
- [116] Japar WMAA, Sidik NAC, Saidur R, Kamaruzaman N, Asako Y, Yusof SNA. The Effect of Triangular Cavity Shape on the Hybrid Microchannel Heat Sink Performance. *CFD Lett.* 2020;12(9):1–14.
- [117] Thermal performance analysis in Sinusoidal–Cavities–Ribs microchannel heat sink with secondary channel geometry for low pumping power application. In: Japar W, Sidik N, Saidur R, Asako Y, Muhammad N, editors. *IOP conference series: Materials science and engineering*. IOP Publishing; 2020.
- [118] Japar WMAA, Sidik NAC, Asako Y. Entropy generation minimization in Sinusoidal Cavities–Ribs microchannel heat sink *via* secondary channel Geometry. *CFD Lett.* 2019;11(7):1–10.
- [119] The effectiveness of secondary channel on the performance of hybrid microchannel heat sink at low pumping power. In: Japar WMAA, Sidik NAC, editors. *IOP conference series: Materials science and engineering*. IOP Publishing; 2019.
- [120] Choi SU, Eastman JA. *Enhancing thermal conductivity of fluids with nanoparticles*. IL (United States): Argonne National Lab; 1995.
- [121] Lyu ZJ, Asadi A, Alarifi IM, Ali V, Foong LK. Thermal and fluid dynamics performance of MWCNT-water nanofluid based on thermophysical properties: An experimental and theoretical study. *Sci Rep.* 2020;10(1):14.
- [122] Xian HW, Sidik NAC, Saidur R. Impact of different surfactants and ultrasonication time on the stability and thermophysical properties of hybrid nanofluids. *Int Commun Heat Mass Transf.* 2020;110:10.
- [123] Sidik NAC, Jamil MM, Japar WMAA, Adamu IM. A review on preparation methods, stability and applications of hybrid nanofluids. *Renew Sustain Energy Rev.* 2017;80:1112–22.
- [124] Abubakar S, Azwadi CN, Ahmad A. The use of $\text{Fe}_3\text{O}_4\text{--H}_2\text{O}_4$ nanofluid for heat transfer enhancement in rectangular microchannel heatsink. *J Adv Res Mater Sci.* 2016;23:15–24.
- [125] Sivakumar A, Alagumurthi N, Senthilvelan T. Effect of serpentine grooves on heat transfer characteristics of microchannel heat sink with different nanofluids. *Heat Transfer-Asian Res.* 2017;46(3):201–17.
- [126] Snoussi L, Ouerfelli N, Sharma K, Vrinceanu N, Chamkha A, Guizani A. Numerical simulation of nanofluids for improved cooling efficiency in a 3D copper microchannel heat sink (MCHS). *Phys Chem Liq.* 2018;56(3):311–31.
- [127] Sarafraz M, Nikkhah V, Nakhjavani M, Arya A. Fouling formation and thermal performance of aqueous carbon nanotube nanofluid in a heat sink with rectangular parallel microchannel. *Appl Therm Eng.* 2017;123:29–39.
- [128] Thansekhar M, Anbumeenakshi C. Experimental investigation of thermal performance of microchannel heat sink with nanofluids $\text{Al}_2\text{O}_3/\text{water}$ and $\text{SiO}_2/\text{water}$. *Exp Tech.* 2017;41(4):399–406.
- [129] Arani AAA, Akbari OA, Safaei MR, Marzban A, Alrashed AA, Ahmadi GR, et al. Heat transfer improvement of water/single-wall carbon nanotubes (SWCNT) nanofluid in a novel design of a truncated double-layered microchannel heat sink. *Int J Heat Mass Transf.* 2017;113:780–95.
- [130] Duangthongsuk W, Wongwises S. An experimental investigation on the heat transfer and pressure drop characteristics of nanofluid flowing in microchannel heat sink with multiple zigzag flow channel structures. *Exp Therm Fluid Sci.* 2017;87:30–9.
- [131] Vinoth R, Kumar DS. Channel cross section effect on heat transfer performance of oblique finned microchannel heat sink. *Int Commun Heat Mass Transf.* 2017;87:270–6.
- [132] Abdollahi A, Sharma RN, Mohammed HA, Vatani A. Heat transfer and flow analysis of $\text{Al}_2\text{O}_3\text{--water}$ nanofluids in interrupted microchannel heat sink with ellipse and diamond ribs in the transverse microchambers. *Heat Transf Eng.* 2018;39(16):1461–9.
- [133] Alfaryjat A, Gheorghian A-T, Nabbat A, Ștefănescu M-F, Dobrovicescu A. The Impact of different base nanofluids on the fluid flow and heat transfer characteristics in rhombus microchannels heat sink. *Sci Bulletin, Ser D.* 2018;80(1):1–14.
- [134] Sarafraz M, Nikkhah V, Nakhjavani M, Arya A. Thermal performance of a heat sink microchannel working with biologically produced silver-water nanofluid: Experimental assessment. *Exp Therm Fluid Sci.* 2018;91:509–19.
- [135] Arabpour A, Karimipour A, Toghräie D. The study of heat transfer and laminar flow of kerosene/multi-walled carbon nanotubes (MWCNTs) nanofluid in the microchannel heat sink with slip boundary condition. *J Therm Anal Calorim.* 2018;131(2):1553–66.
- [136] Tran N, Chang Y-J, Wang C-C. Optimization of thermal performance of multi-nozzle trapezoidal microchannel heat sinks by using nanofluids of Al_2O_3 and TiO_2 . *Int J Heat Mass Transf.* 2018;117:787–98.
- [137] Lyu ZJ, Pourfattah F, Arani AAA, Asadi A, Foong LK. On the thermal performance of a fractal microchannel subjected to water and kerosene carbon nanotube nanofluid. *Sci Rep.* 2020;10(1):16.
- [138] Heat transfer of Al_2O_3 nanofluids in microchannel heat sink. In: Razali A, Sadikin A, Ibrahim S, editors. *AIP Conference Proceedings*. AIP Publishing LLC; 2017.
- [139] Chabi A, Zarrinabadi S, Peyghambarzadeh S, Hashemabadi S, Salimi M. Local convective heat transfer coefficient and friction factor of CuO/water nanofluid in a microchannel heat sink. *Heat Mass Transf.* 2017;53(2):661–71.

- [140] Manay E, Sahin B. Heat transfer and pressure drop of nano-fluids in a microchannel heat sink. *Heat Transf Eng.* 2017;38(5):510–22.
- [141] Status and future prospects of CMOS scaling and Moore's Law-A personal perspective. In: Schwierz F, Liou JJ, editors. 2020 IEEE Latin America electron devices conference (LAEDC). IEEE; 2020.
- [142] Chen Y, Yang C, Kuo C, Chen M, Tung C, Chiou W, editors. Ultra high density SoIC with sub-micron bond pitch. 2020 IEEE 70th electronic components and technology conference (ECTC). IEEE; 2020.
- [143] Schuermans S, Leupers R. Power estimation on electronic system level using linear power models. Switzerland: Springer; 2019.
- [144] Applying the Moore's law for a long time using multi-layer crystal square on a chip. In: El-Aawar H, Sous A, editors. 2019 IEEE XVth international conference on the perspective technologies and methods in mems design (MEMSTECH). IEEE; 2019.
- [145] Wu J, Shen Y-L, Reinhardt K, Szu H, Dong B. A nanotechnology enhancement to Moore's law. *Appl Computational Intell Soft Comput.* 2013;2013:426962.
- [146] Waldrop MM. The chips are down for Moore's law. *Nat N.* 2016;530(7589):144.
- [147] Waldrop MM. More than moore. *Nature.* 2016; 530(7589):144–8.
- [148] Sun S, Narayana VK, Miscuglio M, Kimerling LC, El-Ghazawi T, Sorger VJ. LeAR: A Holistic figure-of-Merit for post-and predicting electronic and photonic-based compute-system evolution. *Sci Rep.* 2020;10(1):1–9.
- [149] Li MY, Su SK, Wong HSP, Li LJ. How 2D semiconductors could extend Moore's law. *Nature.* 2019;567(7747): 169–70.
- [150] Takayama N, Ishizuka J, Yan J. Microgrooving of a single-crystal diamond tool using a picosecond pulsed laser and some cutting tests. *Precis Eng.* 2018; 53:252–62.
- [151] Takayama N, Yan J. Mechanisms of micro-groove formation on single-crystal diamond by a nanosecond pulsed laser. *J Mater Process Technol.* 2017;243:299–311.
- [152] Report MR. Thermal Management Market worth \$12.8 billion by 2025. Mark Mark; 2020. <https://www.marketsandmarkets.com/PressReleases/thermal-management.asp.2020>